Unique benthic foraminiferal communities (stained) in diverse environments of sub-Antarctic fjords, South Georgia

Wojciech Majewski[1], Witold Szczuciński[2], Andrew J. Gooday[3,4]

[1] Institute of Paleobiology, Polish Academy of Sciences, Twarda 51/55, 00-818 Warszawa, Poland
[2] Geohazards Research Unit, Institute of Geology, Adam Mickiewicz University, Bogumiła Krygowskiego 12, 61-680 Poznań, Poland
[3] National Oceanography Centre, European Way, Southampton SO14 3ZH, UK
[4] Life Sciences Department, Natural History Museum, Cromwell Road, London SW7 5BD, UK
Correspondence to: Wojciech Majewski (wmaj@twarda.pan.pl)

Abstract. Sub-Antarctic fjords are among the environments most affected by the recent climate change. In our dynamically changing world, it is essential to monitor changes in these vulnerable settings. Here, we present a baseline study of "living" (rose Bengal stained) benthic foraminifera from fjords of South Georgia, including fjords with and without tidewater glaciers. Their distribution is analyzed in the light of new fjord water and sediment property data, including grain size and sorting, total organic carbon, total sulfur, and $\delta^{13}C$ of bulk organic matter. Four well-defined foraminiferal assemblages are recognized. *Miliammina earlandi* dominates in the most restricted, near-shore and glacier-proximal habitats, *Cassidulinoides* aff. *parkerianus* in mid-fjord areas, and *Globocassidulina* aff. *rossensis* and *Reophax subfusiformis* in the outer parts of fjords. *Miliammina earlandi* can tolerate strong glacial influence, including high sedimentation rates in fjord heads and sediment anoxia, as inferred from sediment color and total organic carbon/sulfur ratios. This versatile species thrives both in the food-poor inner reaches of fjords that receive mainly refractory petrogenic organic matter from glacial meltwater, and in shallow-water coves where it benefits from an abundant supply of fresh, terrestrial and marine organic matter. A smooth-walled variant of *C.* aff. *parkerianus*, apparently endemic to South Georgia, is the calcareous rotaliid best adapted to inner fjord conditions characterized by moderate glacial influence and sedimentation rates and showing no preference for particular sedimentary redox conditions. The outer parts of fjords with clear, slightly warmer bottom water, are inhabited by *G.* aff. *rossensis*. *Reophax subfusiformis* dominates in the deepest-water settings with water salinities ≥ 33.9 PSU and temperatures 0.2–1.4 °C, characteristic for Winter Water and Upper Circumpolar Deep Water. The inner- and mid-fjord foraminiferal assemblages seem specific to South Georgia, although with continued warming and deglaciation they may become more widespread in the Southern Ocean.

1 Introduction

South Georgia (SG) is uniquely positioned between the northern and southern streams of the Antarctic Circumpolar Current (ACC) (Orsi et al., 1995). Since 1925, it has experienced significant warming of the surrounding shallow oceanic waters (Whitehouse et al., 2008) and widespread glacier retreat (Gordon et al., 2008; Cook et al., 2010), changes that coincide with

35 the climatic reorganization of the Southern Ocean caused by the southward shift of the ACC (Gille, 2014) and intensification and southward migration of the Southern Westerly Wind belt (Perren et al., 2020). These major environmental changes will likely continue into the future, strongly affecting marine and terrestrial ecosystems (Constable et al., 2014). They will be particularly evident in fjords (Bianchi et al., 2020) and especially in the highly sensitive sub-Antarctic island of SG, where biological invasions due to increasing vessel traffic are also likely to occur (Frenot et al., 2005). Now is therefore a timely

40 moment to widen our understanding of fjord biota and their links with the local environmental conditions.

This study focuses on foraminifera, a major component of benthic assemblages in marine ecosystems. They are abundant, highly diverse, and many species are preserved in the fossil record. The short life cycle of foraminifera means that they are highly responsive to ecological changes (Jorissen et al., 2009) and therefore particularly valuable for reconstructing paleoenvironments and for monitoring the current state of marine environments (Murray, 1991). Moreover, many calcareous

45 foraminifera secrete their tests in equilibrium with ambient sea water, which makes them useful for reconstructing past water temperatures and salinities using proxies based on analyzing elemental ratios. All these factors make foraminifera an important subject of study.

The primary goal of this research is to document the distribution of different foraminiferal communities inhabiting fjords of SG. Based on new hydrological (water salinity and temperature) and sedimentological data, including grain size and sorting,

50 total organic carbon (TOC), total sulfur (TS), and $\delta^{13}C$ of bulk organic matter, we aim to link these communities with their typical habitats. This will provide a present-day baseline for interpreting fossil records and monitoring future faunal change. Finally, we compare the composition of foraminiferal assemblages inhabiting fjords of SG with those in similar habitats north and south of the ACC. These results may provide insights into likely faunal and ecosystem changes in the Southern Ocean linked to anticipated climate warming.

55 **1.1 Study area**

South Georgia is approximately 170 km long and up to 40 km wide, making it one of the largest sub-Antarctic islands, as well as one of the most remote. It is located within the influence of the ACC (Fig. 1). The southern ACC front wraps anticyclonically around SG before continuing westwards to the north of the island (Thrope et al., 2002). The island is surrounded by a wide shelf composed of continental crust with a long geological history (Curtis et al., 2010) and water-

60 depths rarely exceeding ~300 m (Graham et al., 2008). The closest large land areas are the Falklands and Southern Patagonia, ~1400 km and ~1700 km, respectively, to the west, and the Antarctic Peninsula ~1500 km to the southwest. The smaller archipelagos of the South Sandwich Islands lie about 700 km southeast of SG and the South Orkney Islands about 850 km southwest (Fig. 1).

SG is under the influence of a maritime climate with mean annual temperatures of ~2 °C at Grytviken and annual

65 precipitation of ~1400 mm (Smith, 1960). Weather conditions can be quite variable from year to year, depending on the behavior of the ACC (Cook et al. 2010). SG is strongly affected by Southern Westerly Winds that make its SW shores quite

exposed and NE more sheltered. Due to structural upwelling on the leeward side of the archipelago, the close proximity of oceanic fronts, and local lithogenic sources, waters are rich in nutrients and productive (Davenport, 1995). Coastal water is very cold throughout the year, and in winter and spring it approaches freezing point. In Cumberland Bay, late summer fjord

70 water temperatures decrease from ~2.5 °C to ~1.5 °C and salinity increases from 33–34 PSU to >34.2 PSU near the sea floor at ~250 m water depth (Römer et al., 2014; Geprägs et al., 2016). The water column is stratified, with lower salinity Local Water (LW) at the surface (<33.6 PSU), underlained by water mass resembling Antarctic Surface Waters (AASW), and usually, the deepest water mass approaching the density of Winter Water (WW) and Upper Circumpolar Deep Water (UCDP) (Meredith et al., 2003).

75 SG is a heavily glaciated island, with ice caps and snowfields covering over 50% of the surface. Many fjords are terminated by tidewater glaciers. Out of 103 coastal glaciers, 97% have retreated since the 1950s (Cook et al., 2010). The areas of this study include most of the Cumberland East Bay and West Bay. These are fed at their heads by the Nordenskjöld and Neumayer glaciers, which rank among the largest on the island but show strikingly different retreat rates. While the Nordenskjöld Glacier is almost still (Gordon et al., 2008), retreat rate of the Neumayer Glacier accelerated to nearly 400

80 m/year during 2005–2008 (Cook et al., 2010). The other main sampling area was Stromness Bay. Its catchment is mainly ice-free, and only small cirque glaciers are present. All these bays are located in the center of the NE coast of SG. Additional material was collected in Fortuna Bay and Antarctic Bay, located to the north-west (Fig. 1).

Detailed multibeam swath bathymetry of the studied fjords indicated diverse geomorphology with underwater glacial moraine ridges and distinct basins overprinting large-scale geomorphological features, including troughs that continue out to

85 the shelf edge (Hodgson et al., 2014). The age of these submarine features, both larger- and smaller-scale, remains controversial because marine geological data are sparse (Barnes et al., 2016). The extent of the LGM glaciation is also debated, although an extensive LGM glaciation overriding at least much of the continental shelf (Graham et al., 2008, 2017; Barlow et al. 2016; White et al., 2018) seems more likely than the restriction of LGM glaciers to the fjords (Bentley et al., 2007; Hodgson et al., 2014). The millennial scale sediment accumulation rates are known only from a few sediment cores

90 recovered from the outer parts of Cumberland Bay and vary from 0.1 to 0.2 cm/yr (Berg et al., 2019, 2020; Graham et al., 2017).

1.2 Previous research

Terrestrial ecosystems of sub-Antarctic islands, including SG, have attracted considerable scientific attention, focusing on the impacts of climate change as well as the dispersal of invasive species (Bergstrom and Chown, 1999). However, because

95 of its remoteness, marine ecosystems of SG remain largely understudied (Barnes et al., 2005), despite their important contribution to global and regional biodiversity (Hogg et al., 2011).

Nevertheless, thanks to financing from the whaling industry, SG was the location of one of the classic foraminiferal studies in the Southern Ocean (Earland, 1933, with preliminary papers by Heron-Allen and Earland, 1930, 1932). This work was

based mainly on surface sediments collected during expeditions of the R.R.S. *Discovery* (1925) and R.R.S. *William Scoresby*
100 (1926–1930), mainly at shelf sites but including also some shallower stations in Stromness Bay and Cumberland East Bay
and West Bay. These publications established 49 new foraminiferal taxa, making SG one of the best known areas for
taxonomy of this group in the Southern Ocean. Apart from a recent paper based on samples from the outer shelf and upper
slope (238–354 m water depth) north of SG (Dejardin et al., 2018), and an earlier study that included several sites at similar
upper bathyal depths to the south of SG (Echols, 1971), nothing further has been published on foraminiferal distribution and
105 taxonomy in this region. However, a number of foraminiferal studies have focused on surrounding shelf areas, including the
Falkland Islands and their adjacent shelf (Heron-Allen and Earland, 1932), fjords and channels of Patagonia (Violanti et al.,
2000; Hromic et al., 2006), the South Shetland Islands (Finger and Lipps, 1981; Gray et al., 2003; Majewski, 2005, 2010;
Majewski et al., 2007; Rodriguez et al., 2010), and the Antarctic Peninsula (Ishman and Domack, 1994; Ishman and
Szymcek, 2003; Murray and Pudsey, 2004; Majewski et al., 2016). Research was also conducted in deep-water regions,
110 highlighting foraminiferal gradients across the Drake Passage (Herb, 1971) and the frontal system of the ACC (Mackensen et
al., 1993). Together, these works provide a firm regional background for this study.

2. Material and methods

2.1 Fieldwork

The fieldwork was conducted in fjords located in the central part of the northern coast of SG (Fig. 1 and Table 1) from the
115 *SRV Saoirse* in November and December of 2019. Hydrologic parameters, namely water density, temperature, and salinity
(conductivity), were measured using a CTD48M Memory probe (Sea & Sun Technology GmbH) at 20 stations (Table 1).
Bottom-water measurements for particular stations were based either on direct CTD measurements or extrapolated from the
nearest CTD profile at a similar water depth, since the water properties indicated a uniform water column stratification
throughout each particular fjord (Fig. 2). The salinity is expressed in PSU (practical salinity unit). The classification of local
120 water masses followed mainly a scheme proposed by Orsi et al. (1995), Meredith et al. (2003), Carter et al. (2008), and
Geprägs et al. (2016).

2.1 Sampling

All sediment samples were collected using a Van Veen grab sampler with a sample area of 1000 cm², manufactured by KC
Denmark (model 12.211 matching Norwegian ISO standards). The grab was equipped with inspection windows and rubber
125 plates that opened during descent. After recovering the grab and placing it securely on board, the inspection windows were
opened and excess seawater carefully removed. In the case of over penetration, or if the sediment surface was disturbed (e.g.
due to failure in sealing the grab during the ascent), the sampling was repeated until a good sample was recovered.

For quantitative foraminiferal analyses, the upper 2 cm of sediment was sampled from an area of 63.5 cm², defined by a ring 9 cm in diameter pressed to the sediment surface through one of the inspection windows. Samples for grain size and
130   geochemical analyses were taken from the remaining surface sediment. Additional material was also taken for studies of delicate, gromids (Gooday et al., 2022) and monothalamous foraminifera. At each station, two replicate samples were obtained from two separate deployments of the grab. At stations SG-20 and SG-26, the boat's position could not be maintained due to difficult conditions, resulting in the recovery of replicates from significantly different water depths. In these two cases, both samples were analyzed. Replicates from the remaining stations were archived. In total, 29 samples
135   were fully processed for stained foraminifera: seven from Cumberland East Bay, eight from Cumberland West Bay, three from outer Cumberland Bay, eight from Stromness Bay, two from Antarctic Bay and one from Fortuna Bay (Fig. 1 and Table 1). They were obtained at water depths down to 250 m, i.e. including the deepest parts of the fjords. To study the depth distribution of "live" (stained) foraminifera in the sediment profile, grab samples taken at stations SG-21 and SG-27 were sub-sampled with tubes of 7-cm diameter, providing cores 6 cm long. These were sliced into 1 cm thick intervals directly
140   after recovery.

2.3 Sediment types and grain size analysis

All surface sediment samples were described onboard in terms of sediment type, color, presence of ice-rafted clasts, and macro-biota. Subsamples were taken from 25 grab samples for volumetric grain-size analysis using laser beam diffraction. Prior to the analysis, grains >2 mm in size and organic matter were removed by passing the sample through a sieve and the
145   remaining sediment treated with sodium hexametaphosphate and ultrasound to avoid grain aggregation. The analyses were performed in a Mastersizer 2000 Particle Size Analyzer and the resulting grain-size statistics were calculated with GRADISTAT (Blott and Pye, 2001) using the logarithmic method of moments.

2.4 Geochemistry

Total carbon (TC), TOC and TS analyses were performed using an Eltra CS-500 IR-analyzer at the Faculty of Earth Science,
150   University of Silesia, following standard procedure (Racka et al., 2010). The TOC/TS ratio was used as an approximate indicator of sediment redox, where ratios <1.5 indicate anoxic, 1.5–5 periodically anoxic, and >5 oxic conditions (Berner, 1983). The stable carbon isotopes of bulk organic matter in the sediments were analyzed using a Thermo Electron DeltaV Advantage IRMS with ConFlo II and a Carlo Erba NA1500 Elemental Analyzer at the University of Florida. The data were related to the USGS40 standard (n=28, standard deviation SD=0.081). All carbon isotopic results are expressed in standard
155   delta notation relative to Vienna Peedee Belemnite (VPDB).

2.5 Micropaleontology

Directly after collection, samples were gently washed on a 63-μm-mesh sieve with cold seawater and stained with rose

Bengal (2g/l) and 70% ethanol diluted in sea water. Samples were left to stain for at least two days, washed, and left to dry

for easier transport. The 63–125 μm and >125 μm grain-size fractions were dry-picked. Wherever possible, at least 150

160   stained individuals were picked from each fraction. Samples rich in foraminifera were divided using a dry microsplitter and

all stained tests were picked from the splits. Diversity indices, i.e., Shannon diversity index and dominance were calculated

using PAST4.03 software (Hammer et al., 2001).

Transparent calcareous foraminifera were classified as "living" if at least the final chamber was occupied by brightly red- or

violet-stained cytoplasm (Silva et al., 1996) and opaque agglutinated tests if the cement was intensely stained, especially

165   when wet, or if stained material filled chambers that had been broken open. Porcellaneous foraminifera (miliolids) were

regarded as "living" if material exposed in the aperture was stained or if the test acquired a distinct coloration after re-

wetting (Schönfeld et al., 2012). If samples yielded suspiciously few stained individuals, replicates were checked for

consistency.

All foraminiferal specimens were arranged by taxon on micropaleontological slides and counted. Photographic

170   documentation of specimens typical for each species (Figs. S1–S6) was performed with a Phillips XL20 Scanning Electron

Microscope. The classification scheme used here is that of Loeblich and Tappan (1987) and the WoRMS database (Hayward

et al., 2021). For species of Cassidulinidae, we adopted the latest species-level taxonomy of Majewski et al. (2021), which is

based on molecular data. Specimens are housed at the Institute of Paleobiology, PAS (Warszawa) under the catalogue

number ZPAL F.65.

175   **2.6 Statistics**

As a first step, we selected species that were most characteristic of different environmental settings. The frequencies of

foraminiferal specimens collected from the >125 μm fraction and the entire assemblage (>63 μm; i.e., the >125 plus 63–125

μm fractions), were analyzed individually with Q-mode orthogonal rotated (Varimax) principal component (PC) analysis,

following Malmgren and Haq (1982) and Mackensen et al. (1990), and using a commercially distributed statistics package

180   (SYSTAT 12). Fragile monothalamous foraminifera, such as *Cribrothalammina*, *Pelosina*, and *Vanhoefenella*, which are not

preserved in sub-fossil samples, as well as species never surpassing 1% of the entire fauna and those present only at a single

station, were excluded from the statistical analyses, as were two samples (SG-13 and SG-28) that yielded <80 specimens.

This procedure left 35 and 43 taxa in the >125 μm and >63 μm datasets, respectively.

In the second step, a P-mode PC analysis with the number of factors set at two was conducted and PC loadings were plotted

185   to identify species with similar distributions. Species within distinct groupings were assumed to have similar environmental

requirements, thus belonging to distinct foraminiferal assemblages (Caulle et al., 2014). Combined abundance, expressed as

a percentage of the entire assemblage, was then used for further analysis. Canonical correspondence analysis (CCA) was

conducted using PAST4.03 software (Hammer et al., 2001) in order to investigate the relationship between cumulative

percentages of foraminiferal assemblages (FAs), as well as environmental parameters and sediment properties including

190   water depth, distance to major sediment source, distance to fjord mouth, bottom-water salinity and temperature, TOC, TS, δ^{13}C, mean grain size and sorting.

3   Results

3.1   Fjord hydrology and sediments

3.1.1 Water temperature and salinity

195   The hydrology of the fjords was surveyed during the spring-summer onset of 2019 and revealed a similar pattern of water mass distribution in all the studied fjords (Fig. 2). The surface LW layer was characterized by relatively low salinity (28.4 to 33.6 PSU) and variable temperatures (0.5 to 7.6 °C). This water mass ranged in thickness from ~30 m in the inner part of Cumberland Bay (SG-24) and 26 m in the inner Stromness Bay (SG-18) to 2.4–3.2 m at the outer fjord/shelf stations (e.g. SG-01, SG-02, and SG-21). The lowest salinity (<32 PSU) was found in the surface water of the inner Cumberland West

200   Bay (SG-23, SG-24, and SG-25), which was influenced by meltwater from the tidewater Neumayer Glacier, and in bays supplied with freshwater snowmelt by streams and small rivers (e.g. stations SG-17 and SG-19 in Stromness, and shallow coves in Cumberland Bay: SG-08, SG-12 and SG-22). The lowest temperatures for LW (<1 °C) were noted in the inner parts of Cumberland Bay affected by tidewater glaciers, and the highest (>5 °C) in the inner part of Stromness Bay.
The major fjord water mass was found below LW, down to c. 190–200 m water depth (mwd) (Fig. 2). It was characterized

205   by temperatures that decreased downwards from approximately 2.5 to 0.2 °C, and salinities of between 33.6 and 34 PSU. This water mass was generally similar to AASW and to WW in the deepest parts. The deepest water mass (>200 mwd) was encountered in two parts of Cumberland Bay (Fig. 1), near the fjord mouth and in the innermost western arm of the fjord, which is bounded by a shallow sill, <30 mwd according to *Admiralty Chart 3588* (Fig. 1), and supplied with meltwater by the rapidly retreating Neumayer Glacier. In the outer part of Cumberland Bay (SG-11 and SG-21), the salinity of this deepest

210   water mass increased with depth reaching almost 34.4 PSU, while its temperature slightly increased downward from 0.2 to 1.3 °C, thus corresponding to UCDW. However, in the innermost part of the fjord (SG-22), the water mass below 200 m was colder <0.2 °C and with maximum salinities reaching only 33.86 PSU.
The temperature and salinity of the near-bottom water, which directly influences the benthic biota, ranged from 0.1 to 2.3 °C and 33.5 to 34.35 PSU and varied with water depth (Table 1). The highest temperatures (>1.5 °C) were found at stations

215   shallower than 60 m, located mainly in small bays far away from glacier fronts in Cumberland Bay (SG-22) and Stromness Bay (SG-28, SG-29, and SG-30) but also at SG-13 located close to the front of the Nordenskjöld Glacier. Moderate near-bottom temperatures of 0.75 to 1.5 °C were also found at shallow stations (<60 mwd), as well as at the deepest stations of the outer Cumberland Bay (SG-11 and SG-21, both >240 m deep). The lowest near-bottom water temperatures (0.1–0.6 °C) were encountered at water depths of 90–250 m. Near-bottom waters with a salinity of <33.8 PSU were found at water depths

220   <45 m, and those with values between 33.8 and 34 PSU at depths between 37 and 210 m. In the deepest stations (SG-07, SG-11, and SG-21), water salinity was slightly >34 PSU.

3.1.2 Sedimentology and grain size

Sediments in Antarctic Bay (SG-01 and SG-03) were composed of light grey, poorly sorted glacimarine mud (medium to coarse silt). Sediments in Fortuna Bay (SG-04) were also composed of gray, poorly sorted sandy mud inhabited by
225   Ophiuroidea. In Stromness Bay, sediments mainly comprised poorly-sorted olive-brown to light brown sandy mud. The mean grain size displayed a coarsening offshore trend, from medium silt in inner fjords to very coarse silt/fine sand at the fjord mouth (Fig. 3). Sediment in the central part of Stromness Bay (SG-27) was covered with an algal mat. There was some kelp and abundant plant detritus at station SG-28, located next to Grass Island at the entrance to the Stromness Harbour, the middle branch of Stromness Bay. Here, the sediments below the thin oxidized layer were dark (blackish). At station SG-29
230   (46 mwd), a near-shore location located at the fjord mouth and exposed to ocean swell, sediment was composed of dark, moderately sorted, fine sand.

Samples retrieved from the small coves of Cumberland Bay, i.e., Jason Harbour, King Edward Cove, Sandbugten, and Maiviken, contained olive-gray, poorly sorted muds. In Jason Harbour (stations SG-08 to SG-10) they displayed a subtle, offshore fining trend. Sediments from the restricted, shallow-water settings of Jason Harbour (SG-08) and King Edward
235   Cove (SG-12) were characterized by a circa 1 cm thick light layer with dark (blackish) sediment below. At other stations, the color difference between surface and underlying sediment was much less striking. Fragmented kelp, algal mats, as well as biogenic sediment granules covered the surfaces of sediments retrieved at stations SG-08, SG-09, and SG-12. Sediment collected from deeper water (SG-10) contained more ice-rafted debris (IRD) with gravels up to 6 cm in diameter as well as tubes of Polychaeta.
240   Sediments in the inner part of Cumberland West Bay (SG-23 and SG-24) were light-gray, very loose, and very poorly sorted sandy muds with IRD gravel. In the outer part (SG-32, SG-11, SG-20, and SG-21), they were composed of IRD-rich, poorly sorted sandy muds and muds, colonized by macroscopic benthic organisms (e.g. sponges, Polychaeta). At station SG-31, located west of the shallow sill in the middle part of the fjord, gray and well-sorted coarse sand predominated.

Cumberland East Bay was characterized by gray (SG-13 and SG-16 in the inner part) to olive-gray (SG-06 and SG-07 in the
245   outer part of the bay), poorly sorted, mud to sandy mud (SG-13 next to the glacier). These sediments displayed an offshore grain-size fining trend (Fig. 3). In front of the tidewater glacier (SG-13), the sediment was loose, rich in IRD and inhabited by Ophiuroidea, while in the central part of the fjord Polychaeta-tubes were present more frequently than at other locations. The majority of the analyzed sediment samples were classified as poorly sorted, fine to coarse silt. The sorting was generally correlated with mean grain size, the finer sediments being generally better sorted (Fig. 3). The two outliers were moderately
250   to well sorted sand samples from the swell-affected, shallow-water station SG-29 in Stromness Bay and from SG-31 located on the slope of a sill/moraine in the central part of Cumberland West Bay, a station apparently swept by currents. When

related to the distance along the fjord, samples collected between 7 and 15 km from the fjord mouth (all from Cumberland Bay) included the finest sediments and were slightly better sorted than those from other stations, except for the two outliers (Fig. 3b–c). Subtle trends of coarsening towards both the mouth and head of the fjord (Fig. 3b) may reflect a reduced

255   influence of meltwater discharge with distance from the tidewater glaciers, combined with an increasing winnowing effect of the oceanic currents and swell, and/or increasing relative contribution of IRD in bulk sediments towards the fjord mouth.

3.1.3 TOC and TS

The TC concentrations in the analyzed sediment samples were almost the same as TOC, reflecting the very low total inorganic carbon values (<0.04%). The TOC values varied between 0.23 and 1.1%, except for sample SG-28, located next to

260   Grass Island in Stromness Bay, with a TOC content of 2.92% (Fig. 4). The lowest value (<0.5%) was recorded at all stations located in the inner part of Cumberland Bay, >13 km away from the fjord mouth (Fig. 4A). TOC was elevated (~1%) in the shallow-water settings of King Edward Cove (SG-12), Jason Harbor (SG-08), and stations inside Stromness Bay (SG-17, SG-18, and SG-27). Sediments from stations near the fjord mouths and in the middle of Cumberland Bay yielded intermediate TOC contents.

265   TS varied between 0.07 and 0.38% (Fig. 4). The highest values (>0.2%) were limited to the four shallowest stations (SG-08, SG-12, SG-13, and SG-28), all <40 mwd. Intermediate values between 0.15% and 0.2% were only recorded in the innermost part of Cumberland West Bay (SG-24, SG-31, and SG-32), while the remaining samples yielded the lowest values (<0.15%) (Fig. 4b).

The variations in TOC and TS were not consistent and their ratio was used as an rough indicator of redox conditions (Fig. 5).

270   The highest ratios, typical for mainly oxic sediments, were found in Stromness Bay sediments (all except of SG-29) and in the outer parts of the Cumberland and Antarctic Bay. The lowest values, typical for anoxic sediments, were found in the inner parts of the two main branches of Cumberland Bay, next to terminating tidewater glaciers (Fig. 5a). Two general trends in TOC/TS were observed. Ratios increasing from the fjord mouth towards the fjord head in Stromness Bay and decreased from the fjord mouth towards tidewater glaciers occupying fjord heads in Cumberland Bay (Fig. 5a).

275   ### 3.1.4 δ¹³C of bulk organic matter

The $\delta^{13}C$ in bulk organic matter ranged from –26.06 to –22.42‰ (Fig. 5), and correlated with TOC. The most negative $\delta^{13}C$ values were in samples poorest in TOC, close to the tidewater glacier fronts in the innermost parts of Cumberland Bay. The least negative values were found in samples richest in TOC in the restricted, shallow-water settings of Jason Harbour (SG-08) and King Edward Cove (SG-12), and in Stromness Bay (SG-17, SG-18, SG-27, and SG-28). Two major trends were

280   observed in relation to the distance from the fjord mouth (Fig. 5). In fjords with tidewater glaciers, $\delta^{13}C$ became more negative towards the glaciers at the fjord heads. However, in case of the coves and Stromness Bay, which are not directly affected by glaciers, values increased in the opposite direction. These two trends may represent the progressive mixing of

different types of bulk organic matter, namely (1) material typical for open-marine conditions (δ^{13}C ~–24‰), (2) likely petrogenic organic carbon supplied by glaciers (δ^{13}C ~–26‰), and (3) organic matter derived from fresh terrestrial and

285 marine sources (δ^{13}C ~–23‰). Station SG-15, located in a semi-restricted cove of Sandbugten at a modest distance of ~12 km from the Nordenskjöld Glacier, showed intermediate δ^{13}C values suggesting mixed sources of organic carbon.

3.2 Foraminiferal data

3.2.1 General indices

In the 29 surface samples, a total of 9318 "living", i.e., stained benthic foraminiferal specimens were isolated, including

290 5381 specimens in the >125 μm fraction. They represented >55 species (Figs. S1–S6). The assemblages show significant faunal variability, with numbers of taxa in a single sample (>125-μm fraction) ranging from 4 to 27 (average 14.8) and the Shannon diversity index from 0.79 to 2.58 (average 1.7) (n=29), with standard deviations (SDs) of 6.46 and 0.51, respectively. The Shannon diversity index is the highest in outer fjords at depths of ~100 m or more, and the lowest near the heads of fjords with terminating tidewater glaciers (Fig. 6). Dominance reaches 0.116–0.666 (average 0.30). The numbers of

295 stained specimens per sample (63.5 cm² in area) range from 4 to 1979 (average 186, SD=90.5). The highest abundances are found between 150 and 100 mwd in outer parts of fjords and in the deepest parts of Stromness Bay. The lowest abundances are in the shallow parts of Stromness Bay and at locations near fjords heads (Fig. 2). For the >63 μm fraction, the values of all indices, except dominance, are higher (Fig. 6). The Shannon diversity index ranged from 1.30 to 2.89 (average 1.97). The two short cores taken at stations SG-21 and SG-27 yielded a total of 2810 stained specimens, including 1062 from the

300 >125-μm fraction, representing 47 species. The richest assemblages (>63 μm), in terms of abundances and number of species per sample, were in the upper layers (0–1 cm), totaling 952 and 1724 individuals in cores SG-21 and SG-27, respectively (Fig. 7). The lowest numbers of specimens (36 and 34, respectively) were in the bottom layers (5–6 cm). In the SG-21 sample, the decline in abundances down-core was not uniform, due to a sharp increase in *Stainforthia fusiformis* between 2 and 3 cm below sediment surface.

305 ### 3.2.2 Identification of foraminiferal assemblages

Based on the Q-mode PC analyses, four PC models were selected as best reflecting actual assemblages for both the >125 μm and >63 μm datasets. They explain 81.5 and 84.0% of the total variance in the two datasets, respectively. The calculated PCs are defined by foraminiferal species with large score values (Tables S1 and S2, Fig. 8). They are hereafter referred to as foraminiferal assemblages (FAs) using the name of the dominant taxa, namely the calcareous rotaliids *Globocassidulina* aff.

310 *rossensis* and *Cassidulinoides* aff. *parkerianus,* and the agglutinated *Reophax subfusiformis* and *Miliammina earlandii*. They are the same in both datasets and are therefore not affected by the size-fraction bias.

The P-mode PC analysis was also run on the two datasets separately. The four faunal groups identified in the Q-mode PC analysis could be clearly distinguish in the PC loadings plot for the >125 µm fraction (Fig. 8b). They include different numbers of species, ranging from 4 in the case of the *G.* aff. *rossensis* FA to 16 in the case of the *R. subfusiformis* FA.

315 Importantly, all FAs combine agglutinated and calcareous species. The plot for the >63 µm fraction is less resolved, showing only two groups of taxa (Fig. 8a), indicating that assemblages may be better resolved in the coarser fraction (Jennings and Helgadottir, 1994; Schönfeld et al., 2012; Caulle et al., 2014). Consequently, only the >125 µm results are discussed further.

3.2.3 Spatial distribution patterns of the FAs and their nominative species

Trends in the relative combined abundances of the four FAs as well as in the nominative species alone along the fjord axes

320 are shown in Fig. 9. The *M. earlandi* FA dominated near the fronts of tidewater glaciers and at the most restricted, shallow-water stations. The nominative species, *M. earlandi,* exceeded 35% of the entire assemblage in samples from King Edward Cove near Grytviken and from Jason Harbor (Fig. 6), both small coves with water-depths of ~20 m. *Miliammina earlandi* accounts also for >30% of the entire assemblage at four stations located closest to the fjord heads and tidewater glaciers of Cumberland West Bay and East Bay with water depths of 190 and 28 m, respectively (Fig. 6). In Cumberland West Bay, this

325 species is commonly accompanied by the agglutinated species *Psammosphaera fusca* and *Hippocrepinella hirudinea*, and in Cumberland East Bay (SG-13) by the calcareous species *Gordiospira fragilis* and *Pyrgo patagonica*, all of which contribute to the *M. earlandi* FA (Fig. 8b).

The *C.* aff. *parkerianus* FA dominates in the largest number of samples (Fig. 9). It is common in transitional locations between stations dominated by the three remaining FAs. The nominative *C.* aff. *parkerianus* is the most widespread and

330 abundant species in our dataset. It is represented by two forms (Majewski et al., 2021), a dominant, smooth-walled conical morphotype, assigned by Heron-Allen and Earland (1929) and Earland (1933) to *Ehrenbergina crassa*, and a subordinate porous form resembling *C. parkerianus* sensu Brady (1881), the presence of which is marked on Fig. 9 by red circles. The dominant morphotype reaches the highest percentages, usually well over 50%, far inside Cumberland East Bay and West Bay at water-depths >150 m, as well as at stations SG-08 to SG-10 between 114 and 23 mwd in the middle Cumberland

335 West Bay (Fig. 9). At stations ~50 mwd in outer Stromness (SG-29 and SG-30) and outer Cumberland Bay (SG-22), *C.* aff. *parkerianus* constitutes a moderate share (~30%) of the entire assemblage but with a significant presence of the subordinate porous morphotype.

The *G.* aff. *rossensis* FA dominates near fjords mouths, where foraminifera are relatively abundant and rather rich in calcareous forms (Figs. 6 and 9). *Globocassidulina* aff. *rossensis* strongly dominates its FA, reaching up to 52% in the

340 sample from station SG-26A in outer Stromness Bay and exceeding 40% SG-20A in outer Cumberland Bay. It contributes the highest proportion between ~50 and ~150 mwd in the outer reaches of fjords but also at two stations, SG-15 and SG-06 (51 and 121 mwd, respectively), in central Cumberland East Bay (Fig. 5). *Globocassidulina* aff. *rossensis* is also present at

water-depths >150 m, well inside Cumberland Bay at stations dominated by *M. earlandi* and *C.* aff. *parkerianus*, albeit in low and definitely subordinate numbers.

345 The *R. subfusiformis* FA shows a strong presence in middle and outer Cumberland Bay and throughout Stromness Bay, although not at stations <100 mwd. It is especially important in the deepest fjord settings, but not proximal to glacier fronts (Fig. 6). This FA dominates at stations with the highest species diversity (Fig. 3) and comprises the largest number of species, including agglutinated and calcareous forms (Fig. 5a). Its nominative species, the agglutinated *R. subfusiformis,* is less dominant than those of other FAs (Fig. 6). According to the Q-mode PC analysis (Table S1), *Astrononion echolsi,*

350 *Ammobaculites rostratus,* and to a lesser degree *Cribrostomoides jeffreysii* and *Pullenia subcarinata,* are also important for defining this FA.

3.2.4 Relation between FAs and environmental and sediment properties

CCA was performed in order to explore the relationship between location (water depth, distance to major sediment source, distance to fjord mouth), environmental parameters (water salinity and temperature), and sediment properties (mean grain

355 size and sorting, TOC, TS, δ^{13}C of bulk organic matter) and the cumulative percentages of the four FAs (Table 1 and Fig. 8b). CCA axis 1 explains 70.7% of the variance and axis 2 explains 17.3% (together 88.0%). Most of the variables plot along axis 1, with the *M. earlandi* FA, positive distance to open sea, TS and negative δ^{13}C on the positive side, and the remaining parameters and FAs on the negative side (Fig. 10). The *R. subfusiformis* and *C.* aff. *parkerianus* FAs, as well as water-depth, bottom-water salinity and temperature, showed significant variability along axis 2. The *R. subfusiformis* FA appears to be

360 correlated with elevated salinity, the *G.* aff. *rossensis* FA with higher water temperature, and the *C.* aff. *parkerianus* FA with shallower water depth and increased temperature. However, the correlation is weakest for the *C.* aff. *parkerianus* FA, which also shows the weakest relation with axis 1 of the CCA plot.

4 Discussion

4.1 Data quality

365 Members of the Foraminiferal BIo-MOnitoring initiative (FOBIMO) have proposed several recommendations for monitoring soft-bottom environments using benthic foraminifera (Schönfeld et al., 2012). We aimed to follow their recommendations, such as collecting replicates, rose Bengal staining, and analyzing the >125 μm as well as the 63−125 μm fractions. In some cases, however, we had to adapt the protocol to our field conditions.

Firstly, because sampling time was limited, staining had to be reduced from the recommended 14 days to only a few days. In

370 order to ease penetration of the stain, we gently washed the samples on a 63-μm sieve with cold sea-water, as is routinely done for studying fragile monothalamid foraminifera, before adding rose Bengal in ethanol. Secondly, we sampled the upper 0−2 cm instead of the 0−1 cm interval as recommended by FOBIMO. Due to a frequent presence of a semi-liquid, flocculent

top layer, rich in suspended organic fragments, it was difficult to recognize the sediment-water interface precisely (Fossile et al., 2020). Our motivation was that, for studying robust calcareous and agglutinated species, it is better to sample a thicker

375   rather than a thinner upper sediment layer, especially considering the sharp decline of "living" individuals with depth in similar fjord settings (Majewski, 2013; Fossile et al., 2020). The final and potentially the most critical modification was our use of a Van Veen grab sampler, a device not recommended by Schönfeld et al. (2012). However, our model, equipped with rubber plates that opened during descent reducing the bow wave, proved to be highly efficient and reliable during former sampling for soft testate foraminifera (Majewski et al., 2007; Gschwend et al., 2016). A Kajak sampler was also available

380   during our sampling campaign but it was inefficient.

To provide additional confidence in our procedures, we collected and analyzed two short cores from two of the Van Veen grab samples (SG-21 and SG-27; Fig. 7). In both sediment profiles, we observed abundant and diverse stained assemblages (>125-µm fraction) that were concentrated mainly in the surface layer (Fig. 7). Although the lower distribution limits appeared significantly shallower than on the shelf north of SG (Dejardin et al., 2018), they were comparable to those from

385   similar fjord settings in the South Shetlands (Majewski, 2010) and Spitsbergen (Fossile et al., 2020). Moreover, the 63−125 µm fraction of the SG-21 sub-core revealed a strong subsurface peak in the abundance of *Stainforthia fusiformis* (Fig. 7). The clear distribution pattern of this minute, predominantly infaunal species agrees with its known occupancy of infaunal microhabitats, as reported, for example, by Alve (1994), and confirms that the Van Veen grab samples were relatively undisturbed. Shannon diversity index calculated for >63-µm data was in the range 1.30 to 2.89, encompassing the values of

390   2.29 and 2.36 recorded more offshore by Dejardin et al. (2018). Nevertheless, it is important to note that our surface sampling targeted mainly epibenthic species and that the following discussion is based on the >125 µm data, thereby underestimating the presence of minute, infaunal species, such as *S. fusiformis*.

A final point is that two of the four nominative species for the FAs, *G.* aff. *rossensis* and *C.* aff. *parkerianus,* are phylogenetically closely related (Majewski et al., 2021) and their immature individuals can be difficult to distinguish

395   (Nomura, 1984). However, the color of the cytoplasm when stained was clearly different, more violet in the case of *G.* aff. *rossensis* and more pinkish in *C.* aff. *parkerianus*, making it easy to discriminate between "living" individuals.

4.2 Environmental zones characterized by FAs

We identified four FAs by PC analysis (Fig. 8b). They are very distinctive in terms of species composition and distribution. Figure 9 emphasizes the gradation between FAs dominating proximal to fjord head stations and those showing a stronger

400   presence near the open sea or at greater water depths. According to the CCA (Fig. 10), these four FAs are related to different environmental conditions and sediment properties. In the following sections, we discuss the environmental setting of each.

4.2.1 Inner parts of Cumberland Bay and shallow-water coves: strong glacial influence and sediment anoxia

Restricted areas near tidewater glacier fronts at fjord heads (SG-13, SG-16, SG-24, SG-31) and shallow-water coves (SG-08, SG-12) are dominated by the *M. earlandi* FA (Fig. 9). In these locations, foraminiferal assemblages are impoverished,

405 showing generally low numbers of stained specimens, low to moderate species diversities, and, except at SG-08, a clear dominance of agglutinated forms (Fig. 6). The CCA (Fig. 10) indicates that this FA correlates with (1) large distance from the open sea and, although less clearly, proximity to major sediment sources, (2) strongly negative $\delta^{13}C$ values, and (3) high TS.

The first two correlations are somehow ambiguous as the two types of settings characteristic for the *M. earlandi* FA, i.e.,

410 near the fjord heads and in the coves (Figs. 1 and 6), although both quite restricted, have rather different characteristics. The environments near tidewater glaciers fronts are characterized by variable water depth, relatively coarse glacially-derived sediments that display a fining trend with distance from the sediment source (Fig. 3), and thick layer of brackish, turbid surface water (Fig. 2). In these glacial fjords, sediment TOC values are low (<0.5%; Fig. 4a) and organic-matter $\delta^{13}C$ values strongly negative (Fig. 5b), likely due to the mainly petrogenic source of organic carbon (Berg et al., 2021). Given the

415 climate (high precipitation), mountainous relief, and the susceptibility of rock types to erosion (mudstones and sandstones), it can be expected that sedimentation rates in front of tidewater glaciers are high, in the order of several cm/year, as in the case of similar subpolar fjord systems (e.g. Majewski et al., 2012; Boldt et al., 2013; Streuff et al., 2015). Indeed, preliminary ^{210}Pb dating of a sediment core from station SG-16 (c. 2.5 km away from the front of the Nordenskjöld Glacier) revealed a sediment accumulation rate of ~1.4 cm/yr (Szczuciński, unpublished). In similar depositional environments, the

420 sediment accumulation rate usually exhibits a rapid exponential decrease within the first several km from the glacier front (e.g. Syvitski, 1989; Jaeger and Nittrouer, 1999; Szczuciński and Zajączkowski, 2012). Close to the tidewater glacier fronts, the rates may be in the order of several tens of cm per year. The sediments in glacial fjords are also loose and not compacted, which is also typical for high sedimentation rate conditions. In contrast, sediments in the shallow-water settings of King Edward Cove and Jason Harbor, are among the finest in terms of mean grain size (Fig. 3) and have a thin surfical oxidized

425 lighter mud layer underlain by dark (blackish), probably anoxic sediments. Their sediment accumulation rates were found to be still relatively high, in order of 0.4–0.7 cm/year, as revealed by ^{210}Pb dating (Szczuciński, unpublished). These sediments also yielded high TOC concentrations (>1%, Fig. 4a) and $\delta^{13}C$ ratios that were the least negative in this study (Fig. 5b). These differences seem to reflect different organic-matter sources (Caulle et al., 2014; Jernas et al., 2018), with petrogenic OC dominating near the tidewater glacier fronts and fresher organic matter of mixed origin (both terrigenous and marine)

430 dominating in the coves (Berg et al., 2021).

These fairly substantial differences raise the question of whether *M. earlandi* might comprise several cryptic species, as suggested by molecular data for a related species, *Miliammina fusca* (Pawłowski and Holzmann, unpublished). All stations dominated by the *M. earlandi* FA, however, do have one factor in common, namely elevated TS, roughly ~0.2% (Fig. 4b). The environmental implications of TS alone are difficult to interpret unequivocally but the proportion TOC/TS has been

435 used to evaluate the redox conditions in sediments (Berner, 1983). Thus, although we do not have direct measurements of bottom-water oxygenation or oxygen penetration depths (Caulle et al., 2014), the low TOC/TS ratios suggest oxygen

deficiency at all stations dominated by *M. earlandi* FA (Fig. 5a). It is also in accordance with macroscopic sediment observations in shallow coves sediment samples. This interpretation is consistent with the occurrence of other representatives of *Miliammina* in dysoxic settings (Hayward and Hollis, 1994; Tyszka, 1997; Habura et al., 2006).

440   Earlier studies have shown that *Miliammina earlandi* is not confined to near-shore habitats in the Southern Ocean. This species has a rather complicated taxonomic history, the name having been established by Loeblich and Tappan (1955) to replace the earlier name *M. oblonga,* which was applied incorrectly by Heron-Allen and Earland (1930) and Earland (1933, 1934) (see also p. 53 in Loeblich and Tappan, 1987). The lectotype designated by Loeblich and Tappan (1955) is from 200 m depth, near the shelf edge well to the south of SG. According to Earland (1933), *M. oblonga* (= *M. earlandi*) is 'universally

445   distributed' and 'probably the commonest and most widely distributed rhizopod of the South Georgia area'. The sites where it is common range from 100–200 m, consistent with our new data, but it is also found down to 1752 m. In his subsequent *Discovery* report on the foraminifera of the Falklands area, Earland (1934) concludes that *M. oblonga* (= *M. earlandi*) is 'generally distributed in all areas within the Antarctic convergence and sometimes very common'. The stations he mentioned are at depths of between 244 and 1838 m. *Miliammina earlandi* also occurs in Patagonian fjords, although it is not common

450   (Hromic et al., 2006). Assuming that these records refer to a single species, *M. earlandi* is clearly widely distributed both geographically and bathymetrically in the Southern Ocean and adjacent areas, suggesting that it can tolerate a wide range of conditions.

Adaptability to different habitats seems to be a characteristic of *Miliammina* species more generally. Together with other members of the Rzehakinidae, they inhabit a wide spectrum of both open- and marginal-marine environments (Habura et al.,

455   2006). They are common in salt marshes, mangrove swamps, oligohaline estuaries (Sen Gupta, 1999), persist longer than other foraminifera in marine basins isolated from the sea (Lloyd and Evans, 2002), and dominated in a volcanic caldera less than a decade after significant eruptions (Finger and Lipps, 1981). *Miliammina* species have been also reported from mesohaline habitats (Hayward and Hollis, 1994; Lloyd and Evans, 2002; Habura et al., 2006). In Antarctic waters, *M. arenacea* is associated with corrosive High Salinity Shelf Water (Kennett, 1968; Milam and Anderson, 1981; Ishman and

460   Sperling, 2002) and thrives in areas affected by Antarctic polynya (Capotondi et al., 2018). In SG, highly saline bottom waters were not detected during the present study (Fig. 2) or previous SG surveys (Römer et al., 2014; Geprägs et al., 2016). Instead, the *M. earlandi* FA tends to be associated with rather low salinity (Fig. 10) and its distribution is not restricted to deeper stations (Fig. 9).

This adaptability could confer advantages for *M. earlandi* over other foraminifera at our stations in SG fjords. This may be

465   the last species with a robust test to withstand elevated sediment accumulation rates in fjord heads. It seems to survive anoxia, be able to exploit different food sources, and at the shallow-water stations (SG-08, SG-12, and SG-13), which are at the lower limit of LW influence (Fig. 2), it might experience changes in water salinity and temperature.

It is also worth noting that the *M. earlandi* FA includes different auxiliary species in different areas. In Cumberland West Bay, these are mainly the agglutinated *Psammosphaera fusca* and *Hippocrepinella hirudinea*, and in Cumberland East the

470 calcareous *Gordiospira fragilis* and *Pyrgo patagonica* (Fig. 8b). This difference may be related to different glacial regimes

in these two branches of Cumberland Bay (Gordon et al., 2008).

4.2.2 Mid-fjord settings: transitional conditions

Stations bordering those dominated by the *M. earlandi* FA in the inner reaches of Cumberland Bay (SG-14 and SG-32) show

low to intermediate foraminiferal abundance and diversity (Fig. 6) and a dominance of the *C.* aff. *parkerianus* FA. This is the

475 most widespread FA in our dataset (Fig. 9) and also the most enigmatic. It shows the weakest relation with the main axis 1

on the CCA plot and does not reveal a straightforward correlation with any of the environmental parameters measured in our

study (Fig. 10). The *C.* aff. *parkerianus* FA possibly shows some association with limited water depths and water properties

corresponding with AASW. However, it is less important near fjord mouths, were this water mass predominates (Figs. 1 and

2), therefore an explicit correlation of this FA with AASW is unlikely. The subordinate, porous morphotype of *C.* aff.

480 *parkerianus* (Majewski et al., 2021) is rare or absent far inside Cumberland Bay and in the central part of its western branch

(Fig. 9), suggesting a preference towards more open marine conditions.

Cassidulinoides aff. *parkerianus* is exceptionally well represented throughout Cumberland Bay but not in the innermost part,

where the *M. earlandii* FA dominates, nor at the deepest stations dominated by the *R. subfusiformis* FA or around fjord

mouths, where the *G.* aff. *rossensis* FA predominates. Its strongest presence is in transitional locations between those

485 dominated by these three FAs, so it seems to flourish where conditions are not optimal for other taxa. The abundance of the

smoothly-walled conical morphotype (Majewski et al., 2021) at stations SG-14 and SG-32, adjacent to the most glacier-

proximal stations dominated by the *M. earlandi* FA, suggests that *C.* aff. *parkerianus* FA and its associated rotaliids (Fig. 8b)

are well adapted to inner/middle fjord conditions characterized by moderate sedimentation rates. This would be unique

among *Cassidulinoides* species, which are generally rare or absent in similar settings in the Arctic (Alve et al., 2016),

490 Antarctic (Majewski, 2005) and Patagonia (Hromic et al. 2006). The strong presence of this FA in Jason Harbour, within

Cumberland West Bay (SG-08, SG-09, SG-10), suggests an association with the finest-grained sediments (Fig. 3b). The

TOC/TS ratios at stations dominated by the *C.* aff. *parkerianus* FA cover a wide range (1.8–6.9), suggesting hypoxic to fully

oxic conditions (Berner, 1983), and no strong preference for any particular redox conditions.

4.2.3 Outer-fjord: weak glacial influence, low accumulation rate, relation to bathymetry and water masses

495 The outer-fjord areas are usually characterized by the lowest water turbidity and sedimentation rates (Syvitski, 1989), which

in outer Cumberland Bay are in order of 0.1 to 0.2 cm/yr (Berg et al., 2019, 2020; Graham et al., 2017). Our data show

variable foraminiferal abundances, the highest between 100 and 150 mwd and some of the lowest around 250 mwd, with

high Shannon diversity at the deepest stations (Fig. 6). The *G.* aff. *rossensis* and *R. subfusiformis* FAs dominating in outer-

fjords, are located on the side of axis 1 opposite to the *M. earlandi* FA in the CCA plot (Fig. 10). They correlate with (1)

500 decreased distance to the open sea and increased distance from a major sediment source, (2) less negative $\delta^{13}C$, and (3) low

TS, thus rather high TOC/TS ratios indicating oxic conditions (Berner, 1983). While the *R. subfusiformis* FA seems to be associated with greater water depths and particularly with elevated salinity, the *G.* aff. *rossensis* FA correlates with slightly higher near-bottom water temperature (Fig. 10).

505 The link between the *G.* aff. *rossensis* FA and water temperature revealed by CCA (Fig. 10), suggests that the distribution of this FA coincides with the upper and warmer AASW, which dominates down to 100–150 mwd in Cumberland Bay and throughout the outer Stromness Bay (Fig. 2). However, it is important to note that this FA is abundant only in the central part of Cumberland East Bay and not in Cumberland West Bay (Fig. 9). The front of the Nordenskjöld Glacier is grounded at a relatively shallow water depth of 20–30 m (Hodgson et al., 2014), and its position is relatively stable (Gordon et al., 2008). It is therefore likely delivering less turbid meltwater to Cumberland East Bay, than the rapidly retreating Neumayer Glacier

510 and several land-terminating glaciers in the Cumberland West Bay. As a result, the central part of the eastern branch of Cumberland Bay is less glacially affected, promoting a FA dominated by *G.* aff. *rossensis* rather than by *C.* aff. *parkerianus*. Thus, the *G.* aff. *rossensis* FA appears to flourish in the presence of slightly warmer, clearer water and possibly lower sediment accumulation rates.

The presence of *G.* aff. *rossensis* near fjord mouths at locations distant to glacial and fluvial sediment sources (Fig. 9) is

515 consistent with the distribution of this species in Chilean fjords, where it is an important component of the oceanic and intermediate biofacies but is insignificant in the inner-fjord biofacies (Hromic et al., 2006). Its Antarctic sister species *Globocassidulina biora* (Finger and Lipps, 1981; Majda et al., 2018), on the other hand, seems to be well adopted to habitats proximal to glacier fronts (Majewski, 2005) and beneath ice-shelves (Majewski et al., 2019). However, West Antarctic glaciers deliver significantly less turbid water than rapidly retreating glaciers in SG (Gordon et al., 2008; Cook et al., 2010),

520 which may be one reason for the different distribution patterns near glacier fronts of these two phylogenetically related species.

The *R. subfusiformis* FA is the most species-rich of the four FAs (Fig. 8b). It is abundant throughout Stromness Bay at >100 mwd and in the deepest stations in the middle and outer Cumberland Bay (Fig. 9). According to our CCA, it is strongly correlated with elevated salinity (Fig. 10), pointing to a possible association with WW and UCDW. This would be consistent

525 with observations from the Northern Hemisphere, where *R. subfusiformis* was recorded from locations with high and stable salinities (Höglund, 1947; Thiede et al., 1981; Jernas et al., 2018) and seemed to be more tolerant of a lower quality or quantity of food (Jernas et al., 2018). Two calcareous foraminifera, *Astrononion echolsi* and *Bulimina aculeata,* are also important for this FA (Fig. 8b). They are typical for open marine assemblages in West Antarctica and show an affinity with highly saline Circumpolar Deep Water (Ishman and Domack, 1994, Majewski et al., 2016) that are the least cold

530 (Mackensen, 2001) and one of the oldest (Catalá et al., 2015) water masses in that area.

4.4. Regional comparisons

Foraminifera have been widely studied in fjords, especially in the Arctic (Alve et al. 2016) where there is evidence for strong faunal differences between outer- and inner-fjord locations (e.g. Hald and Korsun, 1997; Korsun and Hald, 1998; Zajączkowski et al., 2010; Fossile et al., 2020) and links with different water-masses (Jennings and Helgadottir, 1994;

535   Jennings et al., 2004). The taxonomic composition of foraminiferal assemblages in Arctic fjords, however, is very different from that in the Southern Hemisphere. For example, in Svalbard and Novaya Zemlya, *Cribroelphidium/Elphidium excavatum* f. *clavata* thrives close to glacier fronts (Hald and Korsun, 1997; Korsun and Hald, 1998), while in SG we encountered only a few empty tests assigned to this genus, and it is also very rare in Antarctica (Majewski and Tatur, 2009). *Cassidulinoides*, so widespread in SG, seems absent in Arctic fjords (Alve et al., 2016), as are species important for other

540   FAs, with the exception of the cosmopolitan *R. subfusiformis* and *Trifarina earlandi/angulosa* (Alve et al., 2016). These strong taxonomic differences between the Northern and Southern Hemispheres make direct faunal comparisons impossible. Previous studies of foraminiferal distributions in fjords located in the same sector of the Southern Hemisphere as SG are limited to Patagonia (Hromic et al., 2006; Korsun et al., unpublished) and Admiralty Bay in South Shetlands (Majewski, 2005, 2010; Majewski et al., 2007). These have revealed clear taxonomic disparities between foraminifera inhabiting

545   different sides of the Drake Passage (Majda et al., 2018; Majewski et al., 2021).

The taxonomic succession observed in the fjords of SG corresponds only in part with observations from Patagonia. Hromic et al. (2006) distinguished three benthic foraminiferal biofacies in fjords and channels of southern Chile. The oceanic sandy biofacies, characterized by elevated organic-matter concentrations and strongly influenced by Pacific water, showed high species richness and high abundances of *G. rossensis* and *Trifarina angulosa*. The intermediate fine-grained biofacies with

550   low organic-matter content and influenced by mixed Pacific and fresh water, was dominated by two calcareous species, *Cassidulina laevigata* and *G. rossensis,* but also included an increased number of agglutinated taxa. The inner-fjord silty biofacies, influenced by cold, low saline water, was characterized by low species diversity and dominated by *Bulimina notovata* and *C. laevigata* (calcareous), together with *Alveophragmium orbiculatum*, *Labrospira kosterensis*, *Recurvoides scitulum*, and *Labrospira jeffreysii* (agglutinated), the last two corresponding to *Veleroninoides scitulus* and *Cribrostomoides*

555   *jeffreysii,* members of the *R. subfusiformis* FA in SG.

It appears, therefore, that the dataset of Hromic et al. (2006) only includes representatives of the two outer-fjord associations from SG, the *G.* aff. *rossensis* and *R. subfusiformis* FAs. Although *M. earlandi,* the nominative taxon of the inner- fjord FA, as well as *C. parkerianus* were encountered in Patagonia, they were not significant species in defining foraminiferal biofacies. The dataset of Hromic et al. (2006), however, did not include the most southerly glaciated fjords in Chilean

560   Patagonia. These were analyzed by Korsun et al. (unpublished), who sampled sea-floor sediments in the Beagle Channel and its tributary fjords, including glaciomarine muds deposited in direct proximity to glacial fronts (Gschwend et al., 2016). They noted *C. parkerianus* as an important species, but it seems morphologically and genetically different from *C.* aff. *parkerianus* in SG (Majewski et al., 2021). The innermost fjord samples in the Beagle Channel region contained only a few foraminifera (~1/10cm^3), which alternated randomly between stations. There was no distinct glacier-proximal assemblage

565   and *Miliammina*, which is so prominent in the most restricted settings in SG, was absent (Korsun et al., unpublished).

In conclusion, it appears that the faunal change is more pronounced along the axes of sub-Antarctic SG fjords, where the *M. earlandi* and *C.* aff. *parkerianus* FAs are well established, than elsewhere around the Scotia Sea. Moreover, there is a disparity between FAs dominant in inner fjord settings, which are found only in SG, and the more biogeographically widespread assemblages inhabiting outer-fjords and shelf sites (Earland, 1933). This is consistent with the contrast between

570   shallow-water SG macrofaunal communities, which show clear Antarctic characteristics, and the more geographically widespread macrofauna in surrounding deep waters which do not (Barnes et al., 2006), further emphasizing the exceptional character of the SG biota (Hogg et al., 2011).

5. Concluding remarks

Since the 1920s, there has been a 0.9–2.3 °C warming in the top 100 m of the water column around SG (Whitehouse et al.

575   2008), as well as air temperature increases since the 1950s coinciding with dynamic glacial retreats (Gordon et al., 2008; Cook et al., 2010). The warming around SG and in the Southern Ocean (Meredith and King, 2005) is also associated with the southward migration of the ACC (Gille, 2014) and shifts in the position and intensity of the Southern Westerly Wind belt (Lamy et al., 2010; Perren et al., 2020). These changes, and their environmental consequences, raise questions regarding the stability of present FA distributions in SG fjords and possible wider-scale reorganization of biogeographic patterns in the

580   Atlantic sector of the Southern Ocean. There is already a broad overlap between foraminiferal species occurring in the fjords of SG and those located to the north and south of the ACC. Among the 60 species recognized in our study, 27 are shared with Chilean fjords (Hromic et al., 2006; Korsun et al., unpublished) and 31 with Admiralty Bay in South Shetlands (Majewski, 2005, 2010, Majewski et al., 2007). However, as discussed above, differences currently exist both at species and assemblage levels between foraminiferal faunas in these regions.

585   The data of Earland (1933) cannot be quantitatively compared with the present study due to different methodologies, but they do show that all major taxa defining the FAs were present in SG during the 1920s (see also Dejardin et al., 2018). Hence, there seems to be no evidence of recent species invasions. Elsewhere, however, the biogeographic barrier of the Drake Passage and the ACC (Orsi et al., 1995) have not prevented faunal migration pulses in and out of Antarctica, especially during past warm periods (Clarke et al., 1992; Majewski et al., 2021). The current warming will likely have major

590   ecological consequences south of the ACC, especially around the Antarctic Peninsula, exposing this region to alien species (Fraser et al., 2018; Convey and Peck, 2019; Avila et al., 2020). This process has already begun (Fillinger et al., 2013; Griffiths et al., 2013) and may be exacerbated by human activity (Frenot et al., 2005; Hughes et al., 2020). With a warming climate and accelerating glacial retreats, conditions in South Shetlands and the Antarctic Peninsula will become more temperate, making them more suitable for the development of foraminiferal assemblages currently typical for SG. Warming

595   is also likely to promote natural faunal dispersal between these areas and SG, with intensified ship traffic (McCarthy et al., 2022) possibly providing an additional vector for the rapid introduction of species. Given the potential for major ecological and biogeographic readjustments in this crucial region of the globe, it is clearly important to continue monitoring for

evidence of increasing faunal connectivity across the ACC, as well as between both sides of the Drake Passage and the unique fjord environments of SG.

600

Supplement. Tables S1, S2, and S3 can be found in the Supplement. Scanning electron micrographs (plates) of all benthic foraminiferal species are shown in Figs. S1 to S6 in the Supplement.

Acknowledgements. We kindly thank for help to RSV *Saorise* crew and the scientific party of the cruise to South Georgia
605 fjords in November-December 2019. Karolina Leszczyńska kindly helped with grain size analyses. The study was funded by Polish National Science Centre grant No. 2018/31/B/ST10/02886.

References

Alve, E.: Opportunistic features of the foraminifer Stainforthia fusiformis (Williamson): evidence from Frierfjord, Norway, J. Micropalaeontol., 13, 24, https://doi.org/10.1144/jm.13.1.24, 1994.

610 Alve, E., Korsun, S., Schönfeld, J., Dijkstra, N., Golikova, E., Hess, S., Husum, K., and Panieri, G.: Foram-AMBI: A sensitivity index based on benthic foraminiferal faunas from North-East Atlantic and Arctic fjords, continental shelves and slopes, Mar. Micropaleontol., 122, 1–12, https://doi.org/10.1016/j.marmicro.2015.11.001, 2016.

Avila, C., Angulo-Preckler, C., Martín-Martín, R. P., Figuerola, B., Griffiths, H. J., and Waller, C. L.: Invasive marine species discovered on non–native kelp rafts in the warmest Antarctic island, Sci. Rep. 10, 1639, https://doi.org/10.1038/s41598-020-
615 58561-y, 2020.

Barlow, N. L. M., Bentley, M. J., Spada, G., Evans, D. J. A., Hansom, J. D., Brader, M. D., White, D. A., Zander, A., and Berg, S.: Testing models of ice cap extent, South Georgia, sub-Antarctic, Quat. Sci. Rev., 154, 157–168, https://doi.org/10.1016/j.quascirev.2016.11.007, 2016.

Barnes, D. K.: Changing chain: past, present and future of the Scotia Arc's and Antarctica's shallow benthic communities, Sci.
620 Mar. 69(S2), 65–89, https://doi.org/10.3989/scimar.2005.69s265, 2005.

Barnes, D. K. A., Linse, K., Waller, C., Morely, S., Enderlein, P., Fraser, K. P. P., and Brown, M.: Shallow benthic faunal communities of South Georgia Island, Polar Biol., 29, 223–228, https://doi.org/10.1007/s00300-005-0042-0, 2006.

Barnes, D. K. A., Ireland, L., Hogg, O. T., Morley, S., Enderlein P., and Sands C. J.:Why is the South Orkney Island shelf (the world's first high seas marine protected area) a carbon immobilization hotspot? Glob. Change. Biol., 22, 1110–1120,
625 https://doi.org/10.1111/gcb.13157, 2016.

Bentley, M. J., Evans, D. J. A., Fogwill, C. J., Hansom, J. D., Sugden, D. E., and Kubik, P. W.: Glacial geomorphology and chronology of deglaciation, South Georgia, sub-Antarctic, Quat. Sci. Rev., 26, 644–677, https://doi.org/10.1016/j.quascirev.2006.11.019, 2007.

Berg, S., White, D., Jivcov, S., Melles, M., Leng, M. J., Rethemeyer, J., Allen, C., Perren, B., Bennike, O., and Viehberg, F.:
630 Holocene glacier fluctuations and environmental changes in Sub-Antarctic South Georgia, Quat. Res., 91, 132–148,
https://doi.org/10.1017/qua.2018.85, 2019.

Berg, S., Jivcov, S., Kusch, S., Kuhn, G., Wacker, L., and Rethemeyer, J.: Compound-specific radiocarbon analysis of (Sub-
)Antarctic coastal marine sediments - potential and challenges for chronologies, Paleoceanogr Paleoclimatol, 35,
e2020PA003890, https://doi.org/10.1029/2020PA003890, 2020.

635 Berg, S., Jivcov, S., Kusch, S., Kuhn, G., White, D., Bohrmann, G., Melles, M. and Rethemeyer, J.: Increased petrogenic and
biospheric organic carbon burial in sub-Antarctic fjord sediments in response to recent glacier retreat, Limnol. Oceanogr., 66,
4347–4362, https://doi.org/10.1002/lno.11965, 2021.

Bergstrom, D. M. and Chown, S. L.: Life at the front: history, ecology and change on southern ocean islands, Trends Ecol.
Evol., 14, 472–476, https://doi.org/10.1016/S0169-5347(99)01688-2, 1999.

640 Berner, R. A.: Sedimentary pyrite formation: An update, Geochim. Cosmochim. Acta, 48, 605–615,
https://doi.org/10.1016/0016-7037(84)90089-9, 1983.

Bianchi, T., Arndt, S., Austin, W., Benn, D. I., Bertrand., S., Cui., X., Faust., J., Koziorowska-Makuch, K., Moy, C., Savage,
C., Smeaton, C., Smith, R., and Syvitski, J.: Fjords as Aquatic Critical Zones (ACZs), Earth-Sci. Rev, 203, 103–145,
https://doi.org/10.1016/j.earscirev.2020.103145, 2020.

645 Blott, S. J. and Pye, K.: Gradistat: A grain size distribution and statistics package for the analysis of unconsolidated sediments,
Earth Surf. Process. Landf., 26, 1237–1248, https://doi.org/10.1002/esp.261, 2001.

Boldt, K. V., Nittrouer, C.A., Hallet, B., Koppes, M. N., Forrest, B. K., Wellner, J. S., and Anderson, J. B.: Modern rates of
glacial sediment accumulation along a 15°S-N transect in fjords from the Antarctic Peninsula to southern Chile, J. Geophys.
Res. Earth Surf., 118, 2072–2088, https://doi.org/10.1002/jgrf.20145, 2013.

650 Brady, H. B.: Notes on some of the Reticularian Rhizopoda of the "Challenger" Expedition. Part III, J. Cell. Sci. 21, 31–71,
https://doi.org/10.1242/jcs.s2-21.81.31, 1881.

Capotondi, L., Bergami, C., Giglio, F., Langone, L., and Ravaioli, M.: Benthic foraminifera distribution in the Ross Sea
(Antarctica) and its relationship to oceanography, Boll. Della Soc. Paleontol. Ital. 57, 187–202,
https://doi.org/10.4435/BSPI.2018.12, 2018.

655 Carter, L., McCave, I. N., and Williams, M. J. M.: Circulation and water masses of the Southern Ocean: a review, in: Antarctic
Climate Evolution, edited by Florindo, F. and Siegert, M., Elsevier, Amsterdam, the Netherlands, 85–114, 2008.

Catalá, T. S., Reche, I., Álvarez, M., Khatiwala, S., Guallart, E. F., Benítez-Barrios, V. M., Fuentes-Lema, A., Romera-
Castillo, C., Nieto-Cid, M., Pelejero, C., Fraile-Nuez, E., Ortega-Retuerta, E., Marrasé, C., and Álvarez-Salgado X. A.: Water
massage and aging driving chromophoric dissolved organic matter in the darkglobal ocean, Global Biogeochem, Cycles, 29,
660 917–934, doi:10.1002/2014GB005048, 2015.

Caulle, C., Koho, K. A., Mojtahid, M., Reichart, G. J., and Jorissen, F. J.: Live (Rose Bengal stained) foraminiferal faunas from the northern Arabian Sea: faunal succession within and below the OMZ, Biogeosciences, 11, 1155–1175, https://doi.org/10.5194/bg-11-1155-2014, 2014.

665 Clarke, A., Crame, J. A., Stromberg, J.-O., and Barker, P. F.: The Southern Ocean benthic fauna and climate change: a historical perspective [and discussion], Phil. Trans. R. Soc. B, 338, 299–309, https://doi.org/10.1098/rstb.1992.0150, 1992.

Constable, A. J., Melbourne-Thomas, J., Conrey, S. P., Arrigo, K. R., Barbraud, C., Barnes, D. K., et al.: Climate change and Southern Ocean ecosystems I: how changes in physical habitats directly affect marine biota, Glob. Chang. Biol., 20, 3004–3015, https://doi.org/10.1111/gcb.12623, 2014.

Convey, P. and Peck, L. S.: Antarctic environmental change and biological responses, Sci. Adv., 11, eaaz0888,
670 https://doi.org/10.1126/sciadv.aaz0888, 2019.

Cook, A. J., Poncet, S., Cooper, A. P. R., Herbert, D. J., and Christie, D.: Glacier retreat on South Georgia and implications for the spread of rats, Antarctic Sci., 22, 255–263, https://doi.org/10.1017/S0954102010000064, 2010.

Curtis, M. L., Flowerdew, M. J., Riley, T. R., Whitehouse, M. J., and Daly, J. S.: Andean sinistral transpression and kinematic partitioning in South Georgia, J. Struct. Geol., 32, 464–477, doi:10.1016/j.jsg.2010.02.002. 2010.

675 Davenport, J.: Upwelling-generated plankton strandlines: Important predictable food sources for seabirds at Husvik, South Georgia, Mar. Biol., 123, 207–217, https://doi.org/10.1007/BF00353612, 1995.

Dejardin R., Kender S., Allen C. S., Leng M. J., Swann G. E. A., Peck V.: "Live" stained benthic foraminiferal living depths, stable isotopes, and taxonomy offshore South Georgia, Southern Ocean: implications for calcification depths, J. Micropalaeontol. 37, 25–71, https://doi.org/10.5194/jm-37-25-2018, 2018.

680 Earland, A.: Foraminifera, Part II, South Georgia, Discov. Rep. 7, 27–138, 1933.

Earland A.: Foraminifera. Part III. The Falklands sector of the Antarctic (excluding South Georgia), Discov. Rep., 10, 1–208, 1934.

Echols, R.J.: Distribution of Foraminifera in sediments of the Scotia Sea area, Antarctic waters, Antarct. Res. Ser., 15, 93–168, https://doi.org/10.1029/AR015p0093, 1971.

685 Fillinger, L., Janussen, D., Lundälv, T., and Richter, C.: Rapid glass sponge expansion after climate-induced Antarctic ice shelf collapse, Curr. Biol., 23, 1330–1334, https://doi.org/10.1016/j.cub.2013.05.051, 2013.

Finger, L. F. and Lipps, J. H.: Foraminiferal decimation and repopulation in an active volcanic caldera, Deception Island, Antarctica, Micropaleontology, 27, 11–139, https://doi.org/10.2307/1485283, 1981.

Fossile, E., Nardelli, M. P., Jouini, A., Lansard, B., Pusceddu, A., and Moccia, D.: Benthic foraminifera as tracers of brine
690 production in the Storfjorden "sea ice factory", Biogeosciences, 17, 1933–1953, https://doi.org/10.5194/bg-17-1933-2020, 2020.

Fraser, C. I., Morrison, A. K., Hogg, A. M., Macaya, E. C., van Sebille, E., Ryan, P. G., Padovan, A., Jack, C., Valdivia, N., and Waters, J. M.: Antarctica's ecological isolation will be broken by storm-driven dispersal and warming, Nat. Clim. Change, 8, 704–708, https://doi.org/10.1038/s41558-018-0209-7, 2018.

695 Frenot, Y., Convey, P., Lebouvier, M., Chown, S. L., Whinam, J., Selkirk, P. M., Convey, P., Skotnicki, M., and Bergstrom, D. M.: Biological invasions in the Antarctic: extent, impacts and implications, Biol. Rev., 80, 45–72, https://doi.org/10.1017/s1464793104006542, 2005.

Geprägs, P., Torres, M. E., Mau, S., Kasten, S., Römer, M., and Bohrmann, G.: Carbon cycling fed by methane seepage at the shallow Cumberland Bay, South Georgia, sub-Antarctic, Geochem. Geophys., 17, 1401–1418,
700 https://doi.org/10.1002/2016GC006276, 2016.

Gille, S. T.: Meridional displacement of the Antarctic Circumpolar Current, Philos. Trans. A Math. Phys Eng. Sci., 372, 20130273, https://doi.org/10.1098/rsta.2013.0273, 2014.

Gooday, A. J., Holzmann, M., Majewski, W., and Pawlowski, J.: New species of Gromia (Protista, Rhizaria) from South Georgia and the Falkland Islands, Polar Biol., 45, 647–666, https://doi.org/10.1007/s00300-022-03017-4, 2022.

705 Gordon, J.E., Haynes, V.M. and Hubbard, A.: Recent glacier changes and climate trends on South Georgia, Glob. Planet. Change, 60, 72–84, https://doi.org/10.1016/j.gloplacha.2006.07.037, 2008.

Graham, A. G., Fretwell, P. T., Larter, R. D., Hodgson, D. A., Tate, A. J., Morris, P., and Wilson, C. K.: A new bathymetric compilation highlighting extensive paleo-ice sheet drainage on the continental shelf, South Georgia, sub-Antarctica, Geochem. Geophys. Geosyst. 9, Q07011, https://doi.org/10.1029/2008GC001993, 2008.

710 Graham, A. G. C., Kuhn, G., Meisel, O., Hillenbrand, C. -D., Hodgson, D. A., Ehrmann, W., Wacker, L., et al.: Major advance of South Georgia glaciers during the Antarctic Cold Reversal following extensive sub-Antarctic glaciation, Nat. Commun., 8, 14798. 2017.

Gray, S. C., Sturz, A., Bruns, M. D., Marzan, R. L., Dougherty, D., Law, H. B., Brackett, J. E., and Marcou, M.: Composition and distribution of sediments and benthic foraminifera in a submerged caldera after 30 years of volcanic quiescence, Deep-
715 Sea Res. II, 50, 1727–1751, https://doi.org/10.1016/S0967-0645(03)00090-0, 2003.

Griffiths, H. J., Whittle, R. J., Roberts, S. J., Belchier, M., and Linse, K.: Antarctic Crabs: Invasion or Endurance? PLoS One, 8, e66981, https://doi.org/10.1371/journal.pone.0066981 ,2013.

Gschwend, F., Majda, A., Majewski, W., and Pawlowski, J.: Psammophaga fuegia sp. nov., a new monothalamid foraminifer from the Beagle Channel, South America, Acta Protozool. 55, 101–110, https://doi.org/10.4467/16890027AP.16.009.4944,
720 2016.

Habura, A. Goldstein, S. T., Parfrey, L. W., and Bowser, S. S.: Phylogeny and ultrastructure of Miliammina fusca: Evidence for secondary loss of calcification in a miliolid foraminifer, J. Eukaryot. Microbiol., 53, 204–210, https://doi.org/10.1111/j.1550-7408.2006.00096.x, 2006.

Hald, M. and Korsun, S.: Distribution of modern benthic foraminifera from fjords of Svalbard, European Arctic, J.
725 Foraminiferal Res., 27, 101–122, https://doi.org/10.2113/gsjfr.27.2.101, 1997.

Hammer, Ø., Harper, D. A. T., and Ryan, P. D.: Past: Paleontological statistics software package for education and data analysis, Palaeontol. Electron., 4, 1–9, 2001.

Hayward, B. W. and Hollis, C.: Brackish Foraminifera in New Zealand: a taxonomic and ecologic review, Micropaleontology, 40, 185–222, https://doi.org/10.2307/1485816, 1994.

730 Hayward, B. W., Cedhagen, T,. Kaminski, M., and Gross, O.: WoRMS Foraminifera: World Foraminifera Database (version 2016-03-01), in: Species 2000 & ITIS Catalogue of Life, 2016 Annual Checklist, edited by Roskov, Y., Abucay, L., Orrell, T., Nicolson, D., Flann, C., Bailly, N., Kirk, P., Bourgoin, T., DeWalt, R. E., Decock, W., De Wever, A., digital resource at www.catalogueoflife.org/annual-checklist/2016, Naturalis, Leiden, the Netherlands, 2021.

Herb, R.: Distribution of recent benthonic foraminifer in the Drake Passage, AGU Antarct. Res. Ser. 17, 251–300, 735 https://doi.org/10.1029/AR017p0251, 1971.

Heron-Allen, E. and Earland, A.: Some new foraminifera from the South Atlantic. Part 2, J. Roy. Micr. Soc. 49, 324–334, https://doi.org/10.1111/j.1365-2818.1929.tb00787.x, 1929.

Heron-Allen, E. and Earland, A.: Some new foraminifera from the South Atlantic. Part 3, Miliammina, a new siliceous genus, J. Roy. Micr. Soc. 30, 38–45, https://doi.org/10.1111/j.1365-2818.1930.tb01474.x, 1930.

740 Heron-Allen, E. and Earland, A.: Foraminifera. Part I. The ice-free area of the Falkland Islands and adjacent seas, Discov. Rep. 4, 291–460, 1932.

Hodgson, D. A., Graham, A. G., Griffiths, H. J., Roberts, S. J., Cofaigh, C. O., Bentley, M.J ., and Evans, D. J.: Glacial history of sub-Antarctic South Georgia based on the submarine geomorphology of its fjords, Quat. Sci. Rev., 89, 129–147, https://doi.org/10.1016/j.quascirev.2013.12.005, 2014.

745 Hogg, O. T., Barnes, D. K. A., and Griffiths, H. J.: Highly diverse, poorly studied and uniquely threatened by climate change: an assessment of marine biodiversity on South Georgia's continental shelf, PLoS One 6, e19795, https://doi.org/10.1371/journal.pone.0019795, 2011.

Höglund, H.: Foraminifera in the Gullmar Fjord and the Skagerak, Zoologiska bidrag från Uppsala, 26, 1–328, 1947.

Hromic, T., Ishman, S., and Silva, N.: Benthic foraminiferal distributions in Chilean fjords: 47 S to 54 S, Mar. Micropaleontol., 750 59, 115–134, https://doi.org/10.1016/j.marmicro.2006.02.001 ,2006.

Hughes, K. A., Pescott, O. L., Peyton, J., Adriaens, T., Cottier-Cook, E. J., Key, G., Rabitsch, W., et. al.: Invasive non-native species likely to threaten biodiversity and ecosystems in the Antarctic Peninsula region, Glob. Chang. Biol., 26, 2702–2716, https://doi.org/10.1111/gcb.14938, 2020.

Ishman, S. E. and Domack, E. W.: Oceanographic controls on benthic foraminifers from the Bellingshausen margin of the 755 Antarctic Peninsula, Mar. Micropaleontol., 24, 119–155, https://doi.org/10.1016/0377-8398(94)90019-1, 1994.

Ishman, S. E. and Sperling, M. R.: Benthic foraminiferal record of Holocene deep-water evolution in the Palmer Deep, western Antarctic Peninsula, Geology 30, 435–438, https://doi.org/10.1130/0091-7613, 2002.

Ishman, S. E. and Szymcek, P.: Foraminiferal distributions in the former Larsen-A Ice Shelf and Prince Gustav Channel region, eastern Antarctic Peninsula margin: a baseline for Holocene paleoenvironmental interpretation, Antarct. Res. Ser. 79, 239–760 260, https://doi.org/10.1029/AR079p0239, 2003.

Jaeger, J.M., Nittrouer, C.A.: Sediment deposition in an Alaskan fjord: Controls on the formation and preservation of sedimentary structures in Icy Bay, J. Sediment. Res., 69, 1011–1026, https://doi.org/10.2110/jsr.69.1011, 1999.

Jennings, A. E. and Helgadottir, G.: Foraminiferal assemblages from the fjords and shelf of eastern Greenland, J. Foraminiferal Res., 24, 123–144, https://doi.org/10.2113/gsjfr.24.2.123, 1994.

765 Jennings, A. E., Weiner, N. J., Helgadottir, G., and Andrews, J. T.: Modern foraminiferal faunas of the southwestern to northern Iceland shelf: oceanographic and environmental controls, J. Foraminiferal Res. 34, 180–207, https://doi.org/10.2113/34.3.180, 2004.

Jernas, P., Klitgaard-Kristensen, D., Husum, K., Koç, N., Tverberg, V., Loubere, P., Prins, M., Dijkstra, N., and Gluchowska, M.: Annual changes in Arctic fjord environment and modern benthic foraminiferal fauna: Evidence from Kongsfjorden,
770 Svalbard, Glob. Planet. Change, 163, 119–140, https://doi.org/10.1016/j.gloplacha.2017.11.013, 2018.

Jorissen, F. J., Bicchi, E., Duchemin, G., Durrieu, J., Galgani, F., Cazes, L., Gaultier, M., and Camps, R.: Impact of oil-based drill mud disposal on benthic foraminiferal assemblages on the continental margin off Angola, Deep-Sea Res. II, 56, 2270–2291, https://doi.org/10.1016/j.dsr2.2009.04.009, 2009.

Kennett, J. P.: The fauna of the Ross Sea. Part 6. Ecology and distribution of the Foraminifera, New Zealand DSIR Bull., 186,
775 1–46, 1968.

Korsun, S. and Hald, M.: Modern benthic foraminifera off Novaya Zemlya tidewater glaciers, Russian Arctic. Arct. Antarct. Alp. Res., 30, 61–77, https://doi.org/10.2307/1551746, 1998.

Lamy, F. , Kilian, R., Arz, H. W. , Francois, J. P. , Kaiser, J. , Prange, M., and Steinke, T.: Holocene changes in the position and intensity of the southern Westerly wind belt, Nature Geoscience, 3, 695–699, https://doi.org/10.1038/NGEO959, 2010,

780 Lloyd, J. M. and Evans, J. R.: Contemporary and fossil foraminifera from isolation basins in northwest Scotland, J. Quat. Sci., 17, 431–443, https://doi.org/10.1002/jqs, 2002.

Loeblich, A. R.; Tappan, H.: Revision of some recent foraminiferal genera, Smithson. misc. collect., 128, 1–37, 1955.

Loeblich, A. R. and Tappan, H.: Foraminiferal Genera and their Classification, Van Nostrand Reinhold Company, New York, USA, 1987.

785 Mackensen, A.: Oxygen and carbon stable isotope tracers of Weddell Sea water masses: new data and some paleoceanographic implications, Deep-Sea Res. I: Oceanogr. Res. Pap., 48, 1401–1422, https://doi.org/10.1016/S0967-0637(00)00093-5, 2001.

Mackensen, A., Grobe, H., Kuhn, G., and Fütterer, D. K.: Benthic foraminiferal assemblages from the eastern Weddell Sea between 68 and 73°S: distribution, ecology and fossilization potential, Mar. Micropaleontol., 16, 241–283, https://doi.org/10.1016/0377-8398(90)90006-8, 1990.

790 Mackensen, A., Fütterer, D. K., Grobe, H., and Schmiedl, G.: Benthic foraminiferal assemblages from the eastern South Atlantic Polar Front region between 35° and 57°S: Distribution, ecology and fossilization potential, Mar. Micropaleontol., 22, 33–69, https://doi.org/10.1016/0377-8398(93)90003-G, 1993.

Majda, A., Majewski, W., Mamos, T., Grabowski, M., Godoi, M. A., and Pawlowski, J.: Variable dispersal histories across the Drake Passage: The case of coastal benthic Foraminifera, Mar. Micropaleontol. 140, 81–94, https://doi.org/10.1016/j.marmicro.2018.02.004, 2018.

Majewski, W.: Benthic foraminiferal communities: distribution and ecology in Admiralty Bay, King George Island, West Antarctica. Pol. Polar Res. 26, 159–214, 2005.

Majewski, W.: Benthic foraminifera from West Antarctic fiord environments: An overview, Pol. Polar Res. 31, 61–82, https://doi.org/10.4202/ppres.2010.05, 2010.

Majewski, W.: Benthic foraminifera from Pine Island and Ferrero bays, Amundsen Sea, Pol. Polar Res. 34, 169–200, https://doi.org/10.2478/popore−2013−0012, 2013.

Majewski, W. and Tatur, A.: A new Antarctic foraminiferal species for detecting climate change in sub-Recent glacier-proximal sediments, Antarct. Sci., 5, 439–448, https://doi.org/10.1017/S0954102009990150, 2009.

Majewski, W., Lecroq, B., Sinniger, F., and Pawlowski, J.: Monothalamous foraminifera from Admiralty Bay, King George Island, West Antarctica, Pol. Polar Res. 28, 187–210, 2007.

Majewski, W., Wellner, J.S., Szczuciński, W., Anderson, J.B.: Holocene oceanographic and glacial changes recorded in Maxwell Bay, West Antarctica, Mar. Geol., 326-328, 67–79, https://doi.org/10.1016/j.margeo.2012.08.009, 2012.

Majewski, W., Wellner, J. S., and Anderson, J. B.: Environmental connotations of benthic foraminiferal assemblages from coastal West Antarctica, Mar. Micropaleontol. 124, 1–15, https://doi.org/10.1016/j.marmicro.2016.01.002, 2016.

Majewski, W., Stolarski, J., and Bart, P. J.: Two rare pustulose/sponose morphotypes of benthic foraminifera from eastern Ross Sea, J. Foraminiferal Res. 49, 405–422, https://doi.org/10.2113/gsjfr.49.4.405, 2019.

Majewski, W., Holzmann, M., Gooday, A. J., Majda, A., Mamos T., and Pawlowski J.: Cenozoic climatic changes drive evolution and dispersal of coastal benthic foraminifera in the Southern Ocean. Scientific Reports 11, 19869, https://doi.org/10.1038/s41598-021-99155-6, 2021.

Malmgren, B. A. and Haq, B. U.: Assessment of quantitative techniques in paleobiogeography, Mar. Micropaleontol., 7, 213–236, https://doi.org/10.1016/0377-8398(82)90003-2, 1982.

McCarthy, A. H., Peck, L. S., and Aldridge, D. C.: Ship traffic connects Antarctica's fragile coasts to worldwide ecosystems, Proc. Natl. Acad. Sci. U.S.A., 119, e2110303118, https://doi.org/10.1073/pnas.2110303118, 2022.

Meredith, M. P. and King, J. C.: Rapid climate change in the ocean west of the. Antarctic Peninsula during the second half of the 20th century, Geophys. Res. Lett. 32, L19604, https://doi.org/10.1029/2005GL024042, 2005.

Meredith, M. P., Watkins, J. L., Murphy, E. J., Ward, P., Bone, D. G., Thorpe, S. E., Grant, S. A., and Ladkin, R. S.: Southern ACC front to the northeast of South Georgia: Pathways, characteristics, and fluxes, J. Geophys. Res., 108(C5), 3162, https://doi.org/10.1029/2001JC001227, 2003.

Milam, R. W and Anderson, J. B.: Distribution and ecology of recent benthonic foraminifera of the Adelie–George V continental shelf and slope, Antarctica. Mar. Micropaleontol., 6, 297–325, https://doi.org/10.1016/0377-8398(81)90009-2, 1981.

Murray, J. W.: Ecology and palaeoecology of benthic foraminifera. Logman Scientific & Technical, London, UK, 1991.

Murray, J. W. and Pudsey, C. J.: Living (stained) and dead foraminifera from the newly ice-free Larsen Ice Shelf, Weddell Sea, Antarctica: Ecology and taphonomy, Mar. Micropaleontol., 53, 67–81, https://doi.org/10.1016/j.marmicro.2004.04.001, 2004.

Nomura, R.: Foraminifera from the raised beach deposits on the east coast of Lutzow–Holm Bay, Antarctica. Mem. Natl. Inst. Polar Res. 28, 219–230, 1983.

Orsi, A. H., Whitworth, T., and Nowlin, W. D.: On the meridional extent and fronts of the Antarctic Circumpolar Current, Deep Sea Res., Part I, 42, 641–673, https://doi.org/10.1016/0967-0637(95)00021-W, 1995.

Perren, B. B., Hodgson, D. A., Roberts, S. J., Sime, L., Van Nieuwenhuyze, W., Verleyen, E., and Vyverman, W.: Southward migration of the southern Hemisphere westerly winds corresponds with warming climate over centennial timescales, Commun. Earth Environ., 1, 58, https://doi.org/10.1038/s43247-020-00059-6, 2020.

Racka, M., Marynowski, L., Filipiak, P., Sobstel, M., Pisarzowska, A., and Bond, D. P. G.: Anoxic Annulata Events in the Late Famennian of the Holy Cross Mountains (Southern Poland): Geochemical and palaeontological record, Palaeogeogr. Palaeoclimatol. Palaeoecol., 297, 549–575, https://doi.org/10.1016/j.palaeo.2010.08.028, 2010.

Rodrigues, A. R., Maluf, J. C. C., De Santis Braga, E., and Eichler, B. B.: Recent benthic foraminiferal distribution and related environmental factors in Ezcurra Inlet, King George Island, Antarctica, Antarct. Sci., 22, 343–360, https://doi.org/10.1017/S0954102010000179, 2010.

Römer M. , Torres, M. , Kasten, S. , Kuhn, G. , Graham, A. G. C. , Mau, S. , Little, C. T. , Linse, K. , Pape, T. , Geprägs, P. , Fischer, D. , Wintersteller, P. , Marcon, Y. , Rethemeyer, J., Bohrmann, G., and Shipboard Scientific Party ANT-XXIX/4: First evidence of widespread active methane seepage in the Southern Ocean, off the sub-Antarctic island of South Georgia, Earth Planet. Sci. Lett., 403, 166–177, https://doi.org/10.1016/j.epsl.2014.06.036, 2014.

Schönfeld, J., Alve, E., Geslin, E., Jorissen, F., Korsun, S., and Spezzaferri, S.: The FOBIMO (Foraminiferal BIo-MOnitoring) initiative – towards a standardised protocol for soft bottom benthic foraminiferal monitoring studies, Mar. Micropaleontol., 94–95, 1–13, https://doi.org/10.1016/j.marmicro.2012.06.001, 2012.

Sen Gupta, B. K.: Foraminifera in marginal marine environments. in: Modern Foraminifera, edited by Sen Gupta, B. K., Kluwer Academic Publishers, Dordrecht, The Netherlands, 141–160, 1999.

Silva K. A., Corliss B. H., Rathburn A. E., and Thunell R. C.: Seasonality of living benthic foraminifera from the San Pedro Basin, California Borderland, J. Foraminiferal Res., 26, 71–93, https://doi.org/10.2113/gsjfr.26.1.71, 1996.

Smith, J.: Glacier problems in South Georgia, J. Glaciol., 3, 705–714, https://doi.org/10.3189/S0022143000018001, 1960.

Streuff, K., Forwick, M., Szczuciński, W., Andreassen, K., Ó Cofaigh, C.: Submarine landform assemblages and sedimentary processes related to glacier surging in Kongsfjorden, Svalbard, Arktos, 1, 14 , 2015. https://doi.org/10.1007/s41063-015-0003-y.

Syvitski, J. P. M.: On the deposition of sediment within glacier-influenced fjords: oceanographic controls, Mar. Geol., 85, 301–329, https://doi.org/10.1016/0025-3227(89)90158-8, 1989.

Szczuciński, W. and Zajączkowski, M.: Factors controlling downward fluxes of particulate matter in glacier-contact and non-glacier contact settings in a subpolar fjord (Billefjorden, Svalbard), IAS Spec. Publ., 44, 369–385, https://doi.org/10.1002/9781118311172.ch18, 2012.

Thiede, J., Ovale, G., Skarbø, O., and Strand, J. E.: Benthonic foraminiferal distributions in a southern Norwegian fjord system:
865   A re-evaluation of Oslo Fjord data, IAS Spec. Publ., 5, 469–495, https://doi.org/10.1002/9781444303759.ch33, 1981.

Thorpe, S. E., Heywood, K. J., Brandon, M. A., and Stevens, D. P.: Variability of the southern Antarctic Circumpolar Current front north of South Georgia, J. Mar. Syst., 37, 87–105, https://doi.org/10.1016/S0924-7963(02)00197-5, 2002.

Tyszka, J.: Miliammina gerochi n. sp. – a middle Jurassic rzehakinid (Foraminiferida) from quasi-anaerobic biofacies, Ann. Soc. Geol. Polon., 67, 355–364, 1997.

870   Violanti, D., Loi, B., Melis, R.: Recent foraminifera from the Strait of Magellan: first quantitative data, Boll. Mus. Regionale. Sci. Nat. Torino, 17, 511–539, 2000.

White, D. A., Bennike, O., Melles, M., Berg, S., and Binnie, S. A.: Was South Georgia covered by an ice cap during the Last Glacial Maximum? Geol. Soc. Spec. Publ., 461, 49, https://doi.org/10.1144/SP461.4, 2018.

Whitehouse, M. J., Meredith, M. P., Rothery, P., Atkinson, A., Ward, P., and Korb, R. E.: Rapid warming of the ocean around
875   South Georgia, Southern Ocean, during the 20th century: Forcings, characteristics and implications for lower trophic levels, Deep-Sea Res. I: Oceanogr. Res. Pap., 55, 1218–1228, https://doi.org/10.1016/j.dsr.2008.06.002, 2008.

Zajączkowski, M., Szczuciński, W., Plessen, B., Jernas, P.: Benthic foraminifera in Hornsund, Svalbard – Implications for paleoenvironmental reconstructions, Pol. Polar Res., 31, 349–375, https://doi.org/10.2478/v10183−010−0010−4, 2010.

880   Table 1. List of stations investigated for this study.

Sample ID	Latitude (54°S)	Longitude (36°W)	Water depth (m)	Date	CTD	Van Veen grab
SG-01	06.200'	58.800'	111	26 Nov	v	v
SG-03	04.250'	56.812'	250	27 Nov	v	v
SG-04	07.658'	47.598'	135	27 Nov	v	v
SG-06	17.299'	28.247'	121	27 Nov	v	v
SG-07	16.052'	26.227'	250	29 Nov	v	v
SG-08	12.038'	34.267'	23	29 Nov	v	v
SG-09	12.044'	34.253'	60	29 Nov		v
SG-10	12.759'	33.677'	114	29 Nov	v	v
SG-11	13.593'	33.525'	240	29 Nov	v	v

SG-12	16.980'	29.977'	21	30 Nov	v	v
SG-13	21.936'	22.486'	28	30.11.19	v	v
SG-14	20.851'	22.749'	155	30 Nov	v	v
SG-15	Sandbugten		51	30 Nov		v
SG-16	21.181'	22.948'	136	1 Dec		v
SG-17	09.533'	41.583'	91.4	2 Dec	v	v
SG-18	10.783'	39.979'	102	2Dec	v	v
SG-20A	13.536'	24.792'	144	3 Dec	v	v
SG-20B	13.586'	25.234'	106	4 Dec		v
SG-21	12.900'	26.963'	252	4 Dec	v	v
SG-22	14.744'	30.395'	45	4 Dec	v	v
SG-23	14.321'	47.206'	202	4 Dec	v	
SG-24	14.653'	42.150'	190	4 Dec		v
SG-25	15.181'	39.446'	170	4 Dec	v	
SG-26A	08.542'	36.592'	155	5 Dec	v	v
SG-26B	08.467'	36.550'	123	5 Dec		v
SG-27	09.372'	38.426'	136	5 Dec		v
SG-28	09.861'	40.175'	37	5 Dec		v
SG-29	10.148'	37.022'	46	5 Dec		v
SG-30	08.337'	37.935'	60	5 Dec		v
SG-31	14.702'	41.702'	188	6 Dec		v
SG-32	15.041'	38.716'	194	6 Dec		v
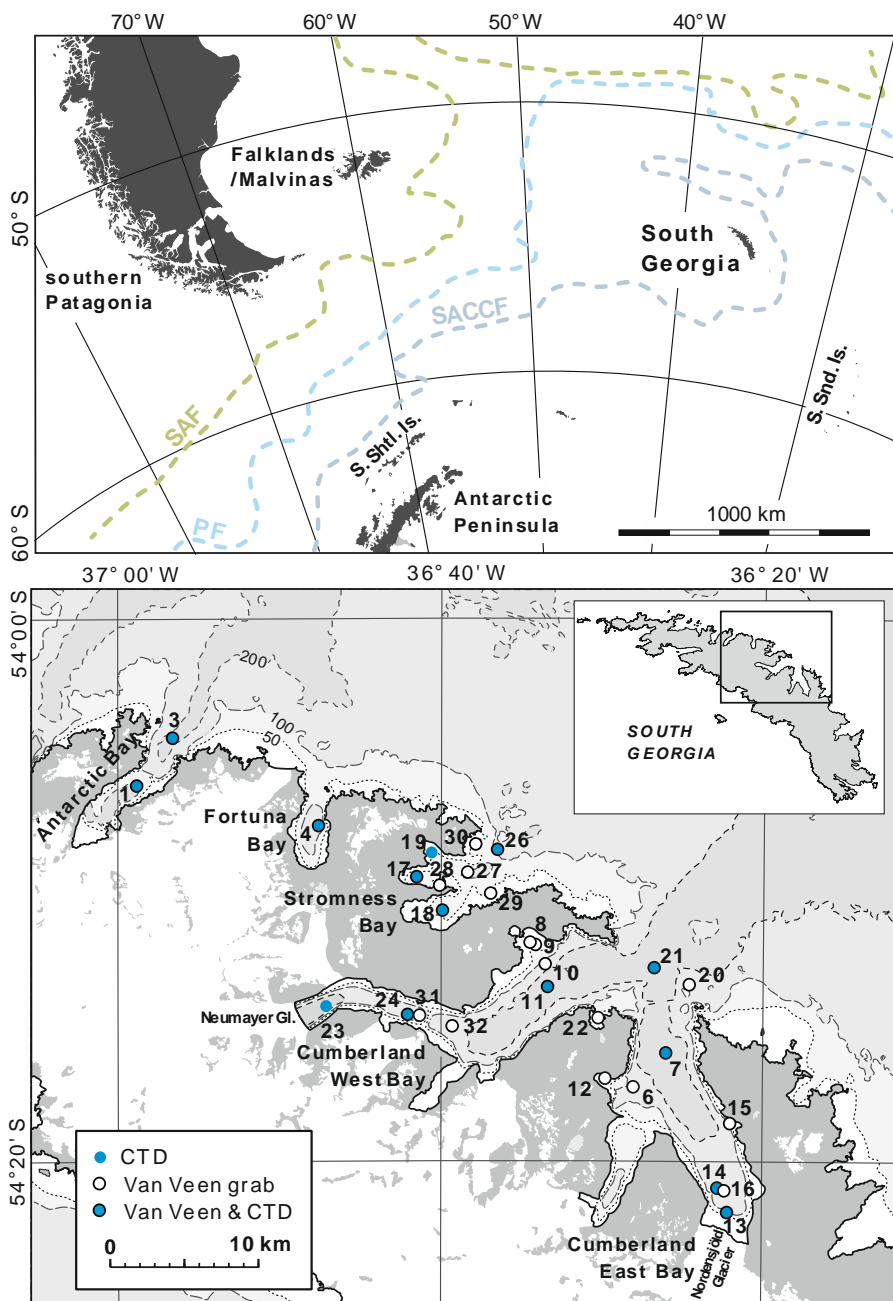
885 **Fig. 1. Study area. Upper map (after https://freevectormaps.com) shows the position of South Georgia in the southwestern Atlantic as well as southern Antarctic Circumpolar Current front (SACCF), the polar front (PF), and the subantarctic front (SAF) after Orsi et al. (1995). Lower map (after *South Georgia and The Shackleton Crossing map* 1 : 200 000, published by British Antarctic Survey in 2017 and *Admiralty Chart 3588, Approaches to Stromness and Cumberland Bays*, 1 : 50 000, second edition, 23rd Jan 2003) shows locations of sampling stations and those CTD stations which data profiles are shown on Fig. 2.**
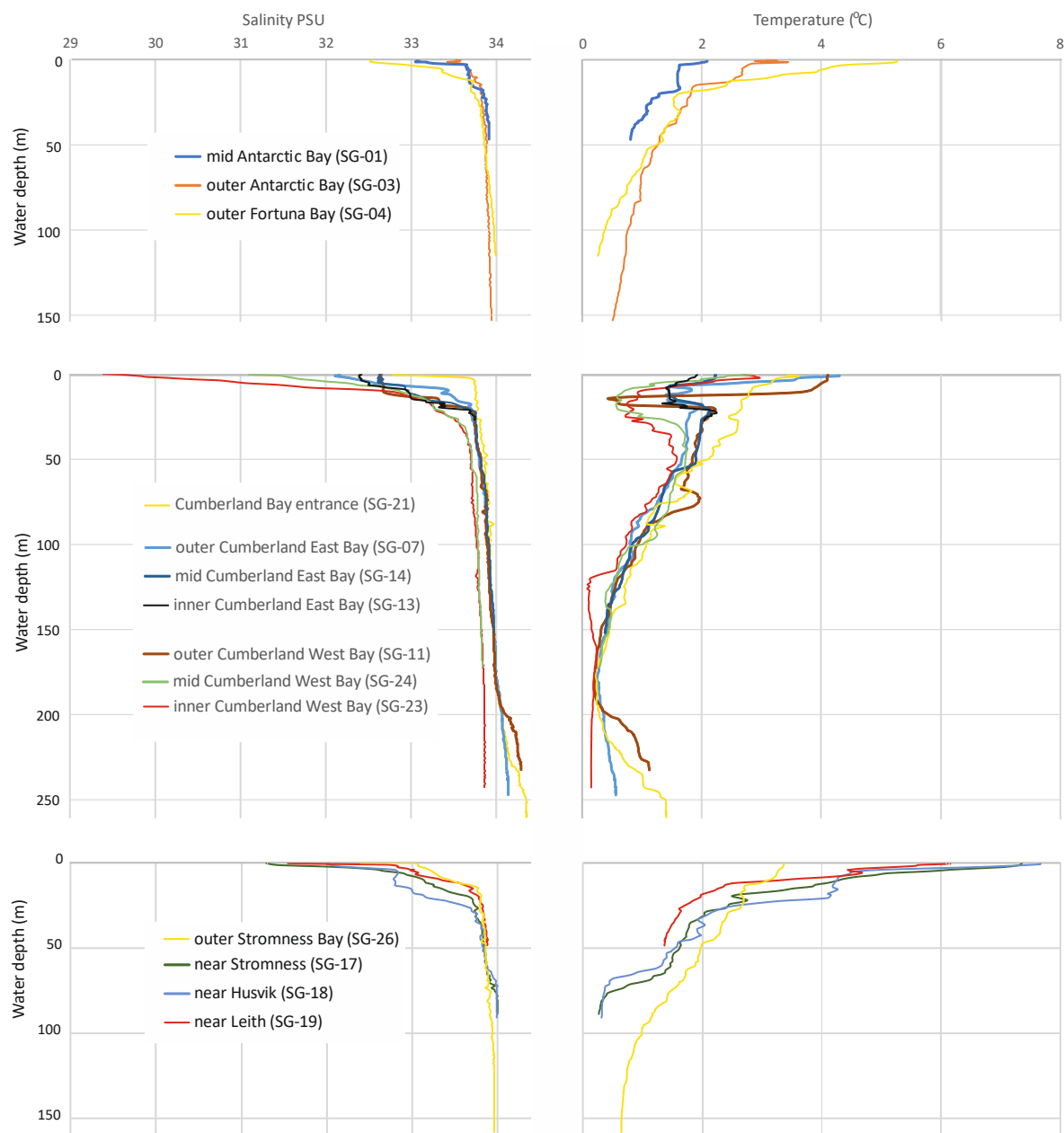
890

Fig. 2. Selected salinity and temperature profiles from Antarctic, Fortuna, Cumberland, and Stromness bays in South Georgia. Locations of the CTD profiles are indicated on Fig. 1 and in Table 1.
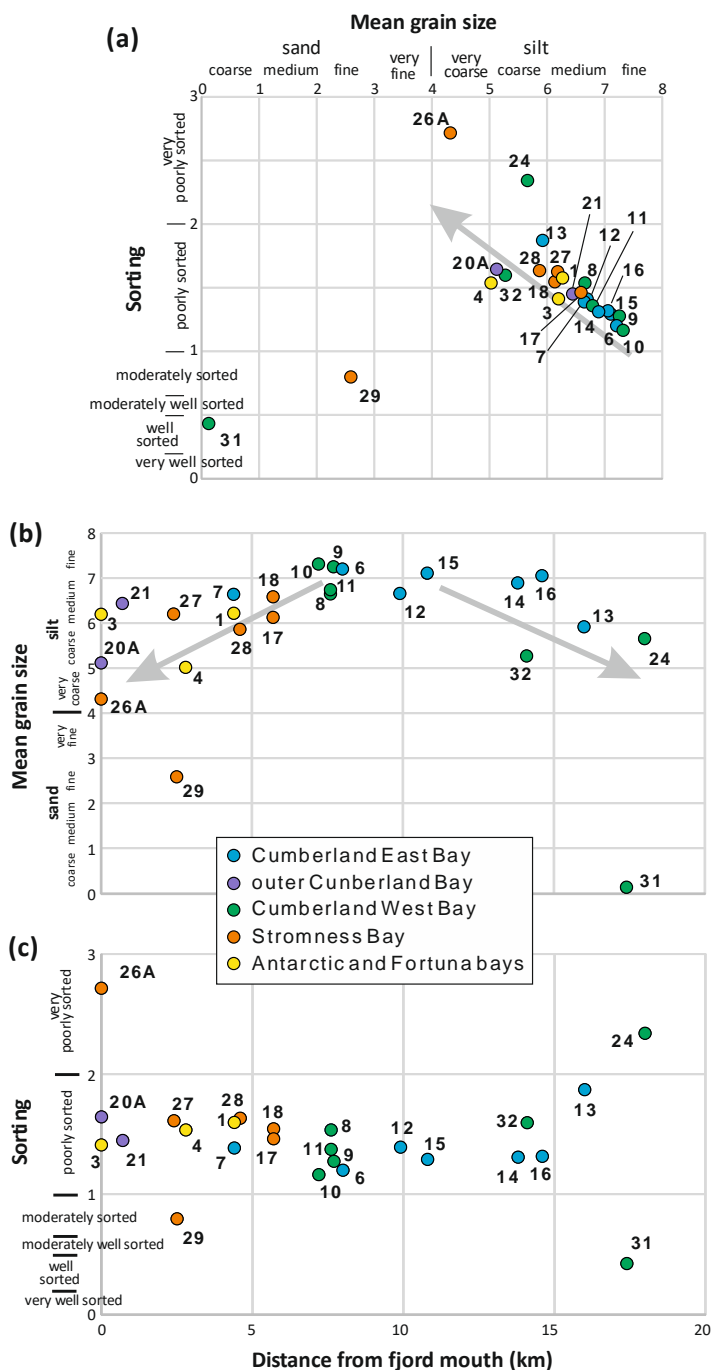
Fig. 3. Sediment mean grain-size vs. sorting expressed in phi scale (a) and the same parameters in relation with distance from fjord
895 **mouth (b and c). Sediment categories are after Blott and Pye (2001). Note trend line to coarser and less sorted sediments in (a), two**
coarsening trends towards fjord mouth and glacier front in (b), and presence of generally better sorted sediments in samples
collected between 7 and 15 km away from fjord mouth in (c).
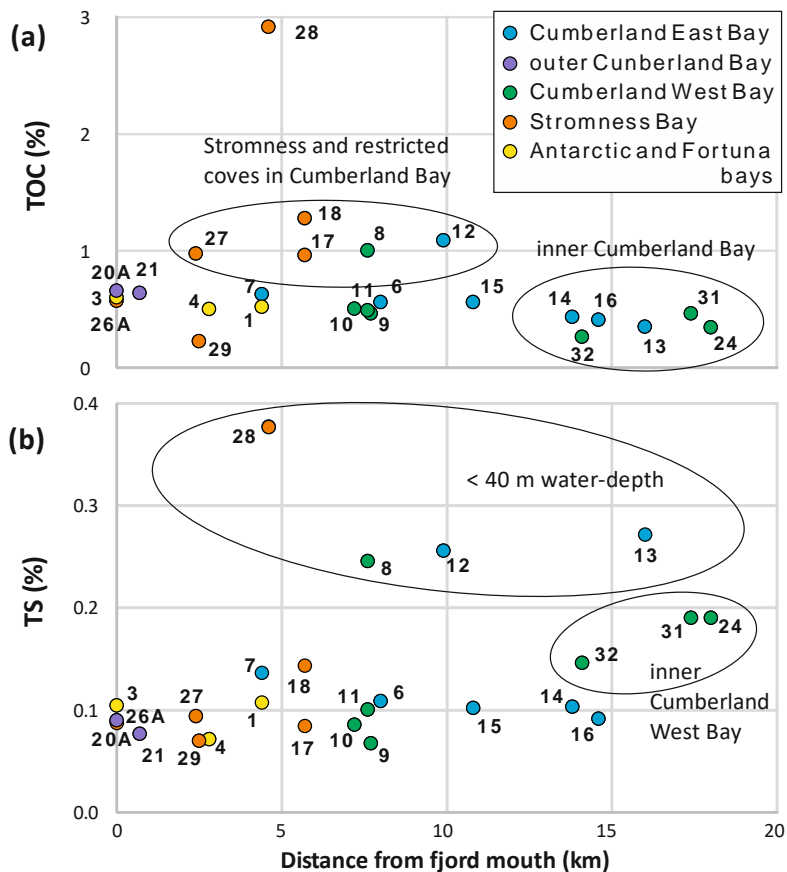
Fig. 4. Total organic carbon (TOC) and total sulfur (TS) in relation with distance from fjord mouth.
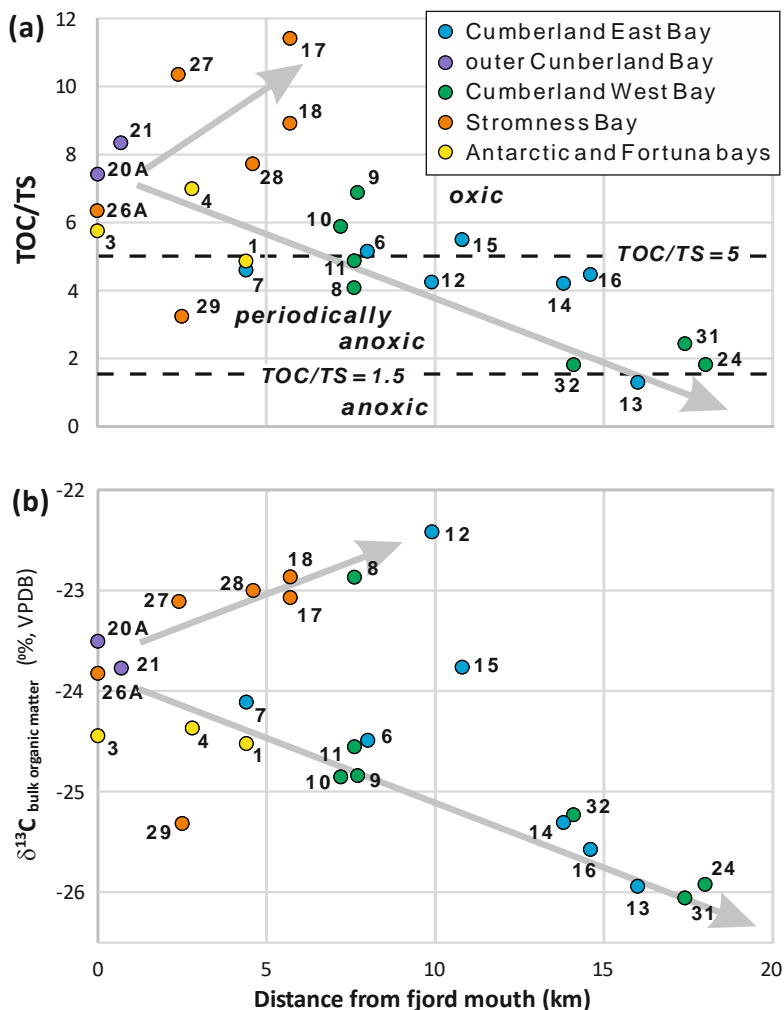
Fig. 5. Total organic carbon to total sulfur ratio (TOC/TS) (a) and carbon stable isotopes of bulk organic matter in the sediments (b) in relation to distance from fjord mouth. Dashed TOC/TS lines at 1.5 and 5 after Berner (1983). Note different trends/mixing lines in (a): towards increasing TOC/TS ratios in Stromness Bay and towards lower ratios in Cumberland Bay, and in (b): towards less negative δ¹³C coves for Stromness Bay and coves and towards more negative values for the main basins of Cumberland Bay affected by tidewater glaciers.

905
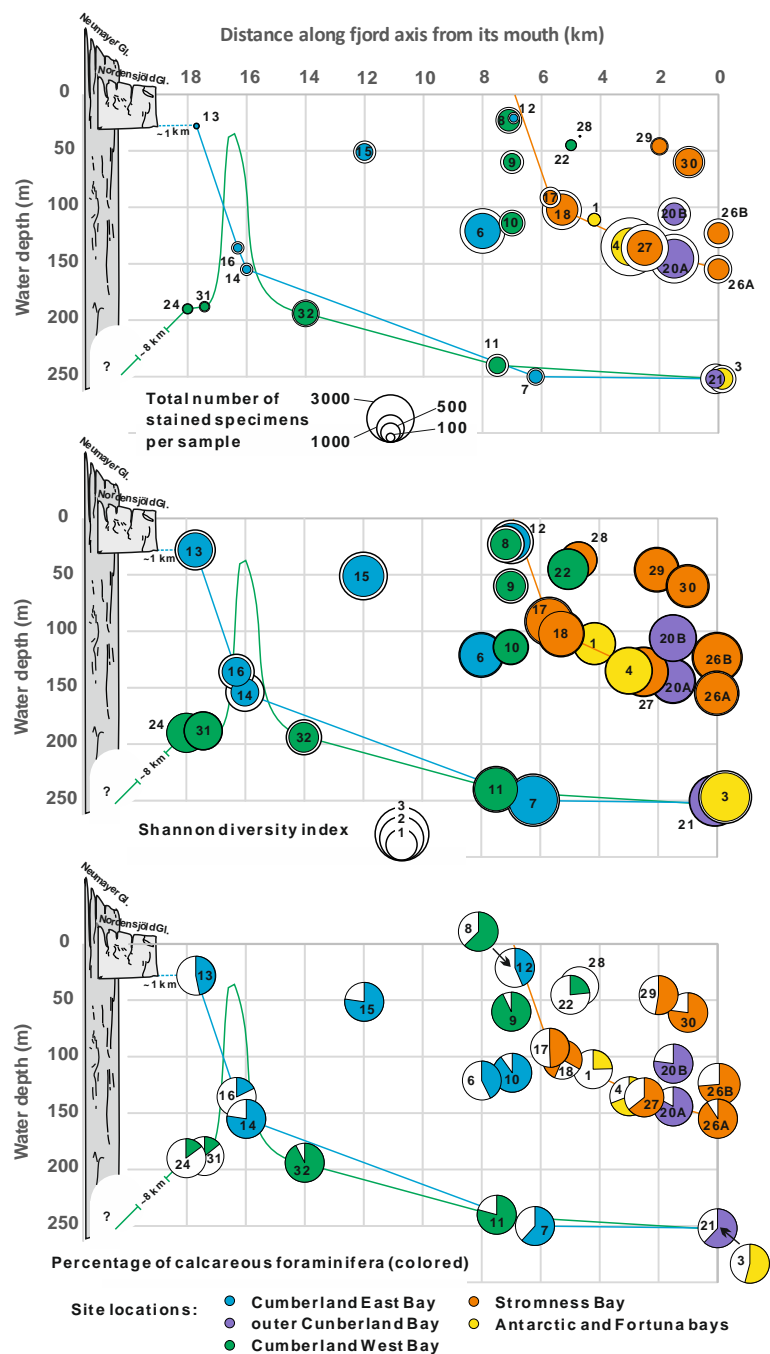
Fig. 6. General indices of benthic foraminiferal assemblages plotted against bathymetry and distance to open sea along fjord axes. Different colors represent locations in various fjords. Color lines show simplified bathymetric profiles for Stromness Bay, Cumberland East Bay, and Cumberland West Bay. Colored circles are for the >125 μm fraction, white circles in two upper graphs are for the >63 μm fraction.

910
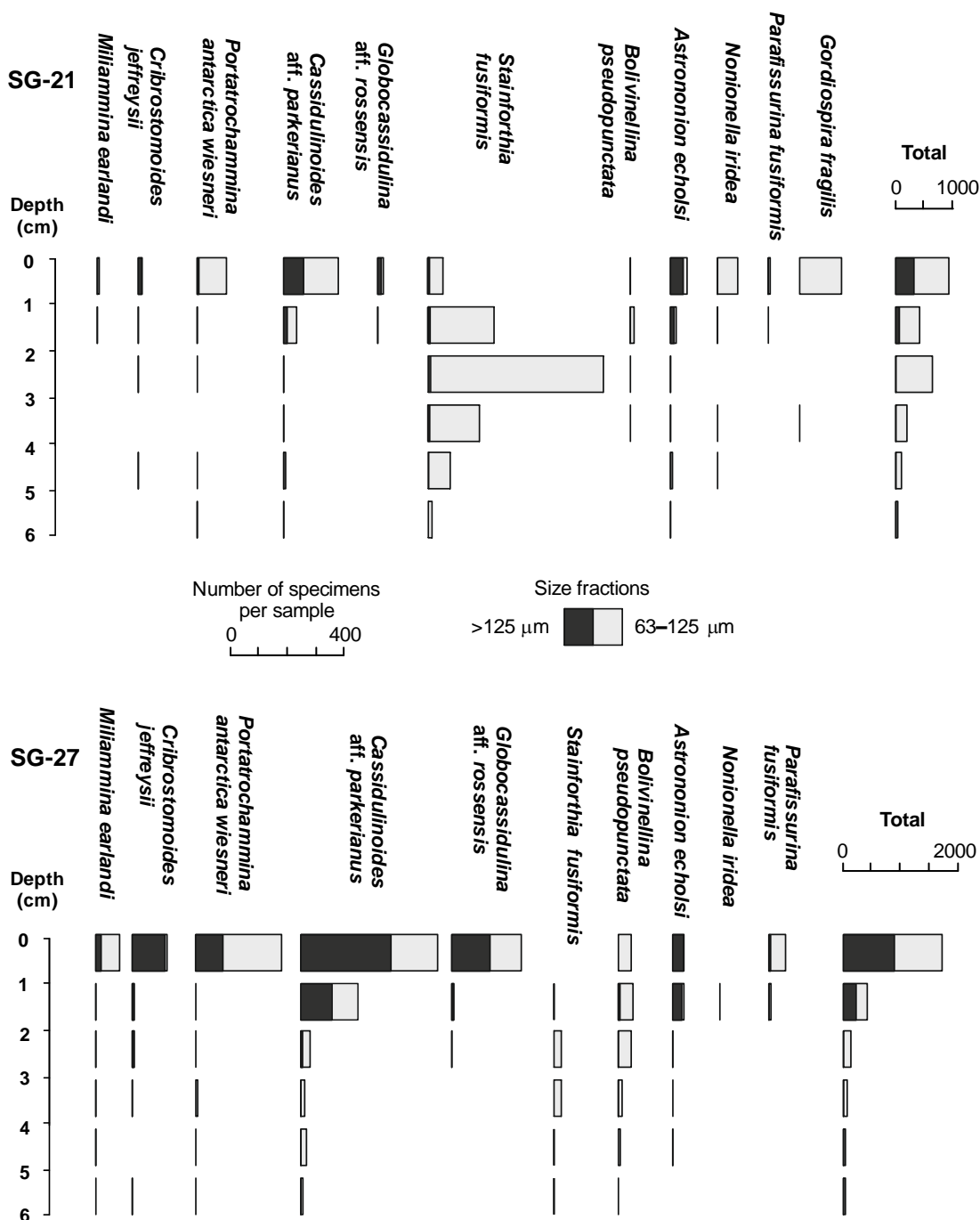
Fig. 7. Abundances in numbers per sample of stained foraminifera in two short cores taken at stations SG-21 and SG-27. Note different scales for specific and total abundances.
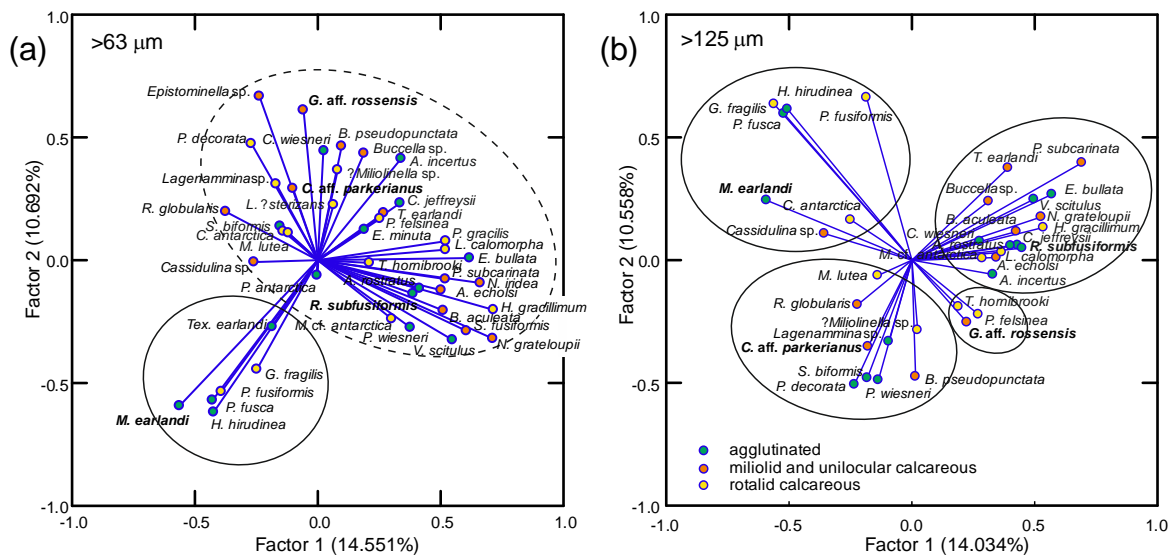
Fig. 8. Plots of the factor loadings for the P-mode PC analysis, showing distribution of different foraminifera species for the >63 µm (a) and >125 µm (b) datasets. The PC model was based on relative abundances of the more important species, i.e. >1% of total assemblage in at least one sample. Samples SG-13 and SG-28, which yielded low specimen numbers, were not included. Nominative species for each FA are in bold. Note much better resolution of the four FAs for the coarser fraction.
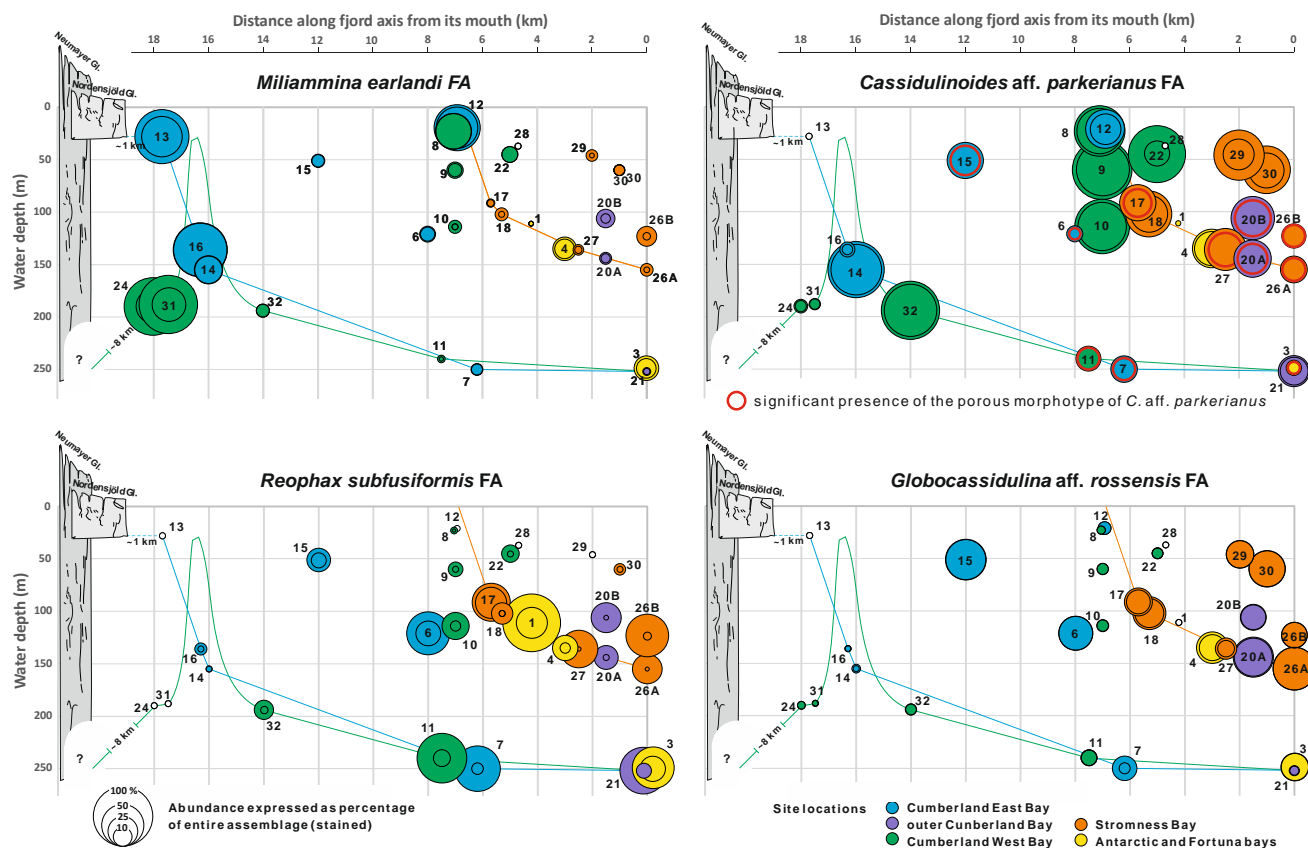
920 **Fig. 9. Cumulative percentages of the four species groups (FAs) defined by the PC analysis in relation to the entire >125 μm assemblages plotted against bathymetry and distance along fjord axis to its mouth. Smaller circles indicate percentages of the nominative species. All graphs at the same scale. Different colors represent locations in various fjords. Color lines show simplified bathymetric profiles for Stromness Bay, Cumberland East Bay, and Cumberland West Bay.**
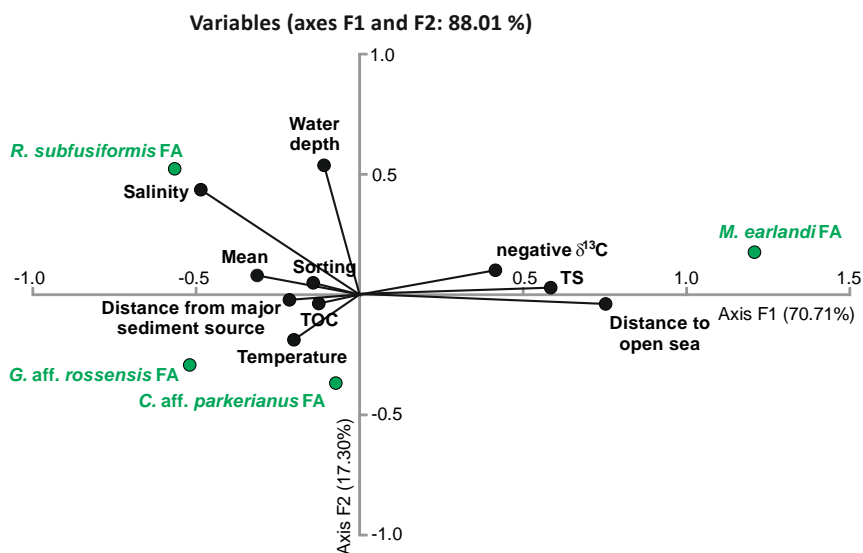
925 **Fig. 10. CCA plot of the faunal assemblages (FAs) defined by PCA (in green) with various parameters (in black), including: location (water depth, distance from major sediment source and distance to open sea), environmental parameters (salinity and temperature), and sediment properties (total organic carbon (TOC) and its isotopic composition, total sulfur (TS), mean grain size and sorting).**